AD-A138 099 DEPENDENCE OF HOLOGRAPHIC GRATING FORMATION UPON INTERFERENCE PATTERN ORI..(U) AIR FORCE INST OF TECH WRIGHT-PATTERSON AFB OH SCHOOL OF ENGI.. C L MATSON 1/2

UNCLASSIFIED DEC 83 AFIT/GEO/EE/83D-4 F/G 20/6 NL

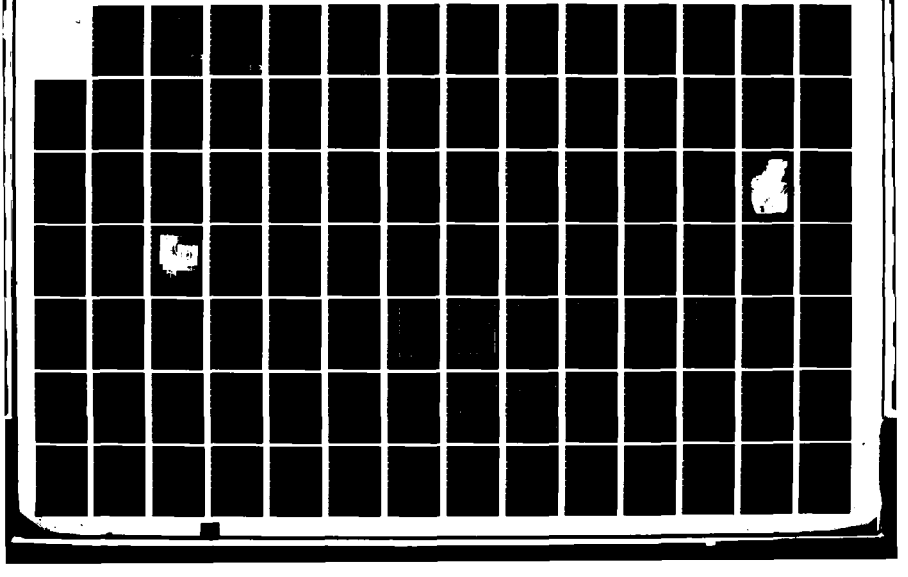

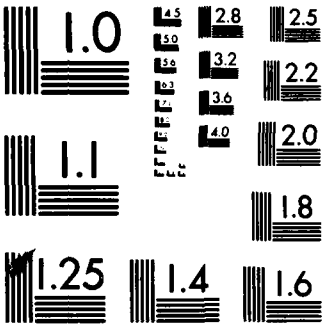

MICROCOPY RESOLUTION TEST CHART
NATIONAL BUREAU OF STANDARDS-1963-A

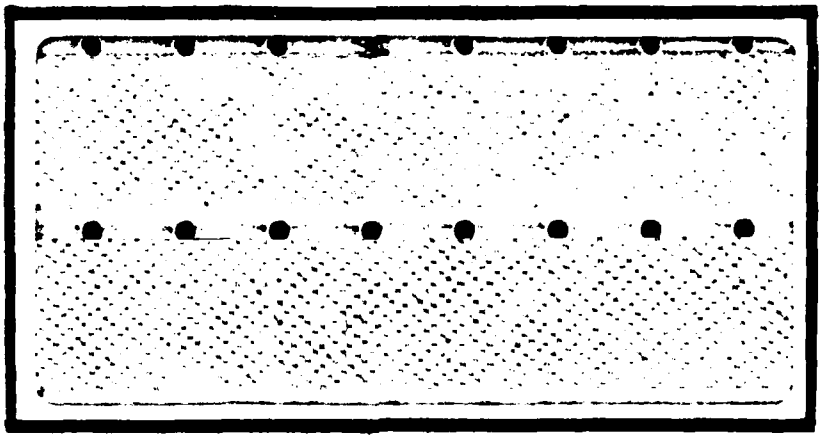

DEPARTMENT OF THE AIR FORCE

AIR UNIVERSITY

AIR FORCE INSTITUTE OF TECHNOLOGY

Wright-Patterson Air Force Base, Ohio

AFIT/GEO/EE/83D-4

DEPENDENCE OF HOLOGRAPHIC GRATING FORMATION UPON INTERFERENCE PATTERN ORIENTATION IN BISMUTH SILICON OXIDE

THESIS

AFIT/GEO/EE/83D-4 Charles L. Matson
2nd Lt. USAF

AFIT/GEO/EE/83D-4

DEPENDENCE OF HOLOGRAPHIC GRATING FORMATION UPON INTERFERENCE PATTERN ORIENTATION IN BISMUTH SILICON OXIDE

THESIS

Presented to the Faculty of the School of Engineering
of the Air Force Institute of Technology
Air University
in Partial Fulfillment of the
Requirements for the Degree of
Master of Science

by
Charles L. Matson, B.S.
2nd Lt USAF
Graduate Electro-Optics
December 1983

Acknowledgments

Dr. Charles L. Woods of Rome Air Development Center suggested this topic. I wish to thank him for all the time he spent guiding, teaching, and encouraging me throughout the course of the research.

I also wish to thank Dr. Michael Salour and Ms. Terry Bruno for the long hours they spent with me in the laboratory. Special thanks are also due to Dr. Jacques Ludman for making it possible for me to spend the summer at RADC, and to Dr. Cardinal Warde for his conversations with me concerning the research.

I wish to express my gratitude to my thesis advisor, Dr. Vaqar Syed, for his guidance and encouragement during the writing of the thesis, and to Dr. Theodore Luke for his penetrating comments concerning the thesis.

My wife, Dawn, deserves special thanks for being a special friend and also helping me produce the final draft of the thesis.

Finally, I wish to thank the Lord Jesus Christ for His peace and love in my life that gave me the strength necessary to finish this project, and for the meaning He gives to my entire life.

Contents

List of Figures

List of Tables

ABSTRACT

Bismuth silicon oxide (BSO) is a material which shows good promise for use as a reusable holographic storage medium, with cycle times on the order of milliseconds. When operated without an applied voltage, fringe patterns are weakly recorded through a space charge field in the crystal equally well for all fringe orientations. The fringes are recorded much more strongly in the crystal when a f· d of 5 to 10 kV/cm is placed across the crystal; however, streng of fringe storage becomes dependent on the orientation of the f . s upon the crystal. Thus, it is necessary to determine how the strength of fringe storage depends upon the fringe angle to fully utilize the advantage of using an applied voltage to enhance crystal performance.

A particularly simple hologram is made by interfering two plane waves, producing a sinusoidal interference pattern with parallel fringes. By measuring diffraction efficiencies of thick birefringent phase diffraction gratings formed in BSO by recording a sinusoidal interference pattern for a variety of fringe angles, the effect of fringe orientation upon fringe storage can be determined. This is the approach used in this thesis to analyze the fringe angle dependence of fringe storage in BSO.

Angular dependence of diffraction efficiencies were obtained for several values of parameters such as applied voltage, modulation coefficient of the sinusoidal pattern, polarization of diffracted beam, exposure times, and spatial frequency. It was theorized that the effect of the voltage on fringe storage would scale sinusoidally

as a function of the angle between the applied field and the fringe pattern. This theory proved to be valid for short to intermediate exposure times for the scaling of the growth rates of the space charge field. Polarization of the diffracted beam also significantly affected fringe storage of the BSO crystal. An index ellipsoid calculation based on an approximation for the space charge field in the crystal gave qualitative agreement for the magnitude of the space charge field growth.

I. INTRODUCTION

A. BACKGROUND

The technique of holography was invented by Dennis Gabor in 1947 to help improve the resolution of the electron microscope. However, to this day, holography has not been successfully applied in this area. Many other applications of holography have been discovered, though, including non-destructive testing, optical memory storage, and holographic optical elements. The types of storage media available on which to record holograms play an important role in determining whether holography can be applied in a given situation. In particular, many uses of holography, such as optical implementation of dynamic matched filtering, require storage media which can record holograms in real time situations. Unfortunately, many of the available storage media which possess fast response times and that can be erased lack other desirable properties like good photosensitivity or high resolution, and media which have these desirable properties do not have fast response times and cannot be erased.

A group of materials (called photorefractives) do exist which have fast response times and are erasable, and also have some of these other desirable properties. These materials record holograms by undergoing refractive-index changes through optical illumination (the photorefractive effect). Members of this group include ferroelectric

crystals such as lithium niobate (LiNbO) and barium titanate (BTO), along with paraelectric crystals such as bismuth germanium oxide (BGO), and bismuth silicon oxide (BSO). BTO and BSO, which are the two primary candidates out of this group for holographic storage use, possess important differences. BTO is capable of diffraction efficiencies of up to or greater than one, but has response times of one to ten seconds typically and can cost tens of thousands of dollars at this time. BSO, on the other hand, has much lower diffraction efficiencies, but can have response times on the order of milliseconds and is available for less than a tenth of the price of BTO. Because BSO has such fast response times and is much cheaper, along with possessing photographic sensitivity (100-300 uJ/cm2) at the argon green (514.5 nm) laser line, it was chosen for the study reported in this thesis.

BSO can be used as a holographic storage medium when operated in the transverse electro-optic configuration as first reported by J.P. Huignard and F. Micheron (Ref. 1). This configuration is shown in Figure 1, where the applied voltage usually ranges from 1 to 10 kilovolts, resulting in applied fields of 1 to 10 kilovolts/cm since the width of a BSO crystal is typically 1 cm. Light interference patterns such as the sinusoidal pattern shown in Figure 1 by the periodic spacing of lines are recorded in the crystal as described below. Electrons are photoexcited from impurity levels in the crystal into the conduction band, with the rate of production of excited electrons proportional to the local intensity of the interference pattern in the crystal. These electrons, which are now free to migrate in the crystal, move in the general direction of the applied field and eventually become retrapped. As this process continues, the trapped

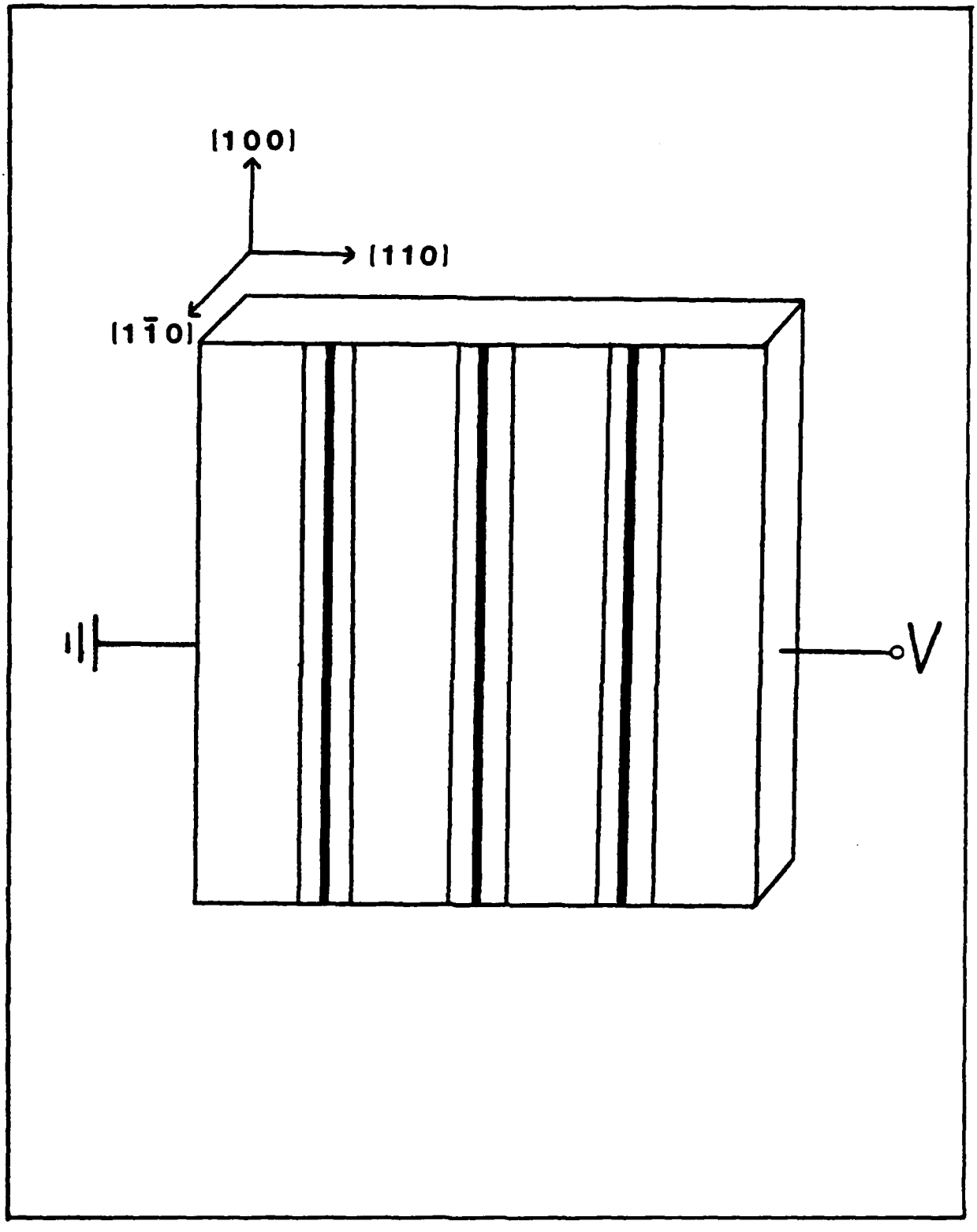

Figure 1. BSO crystal in tranverse electro-optic configuration with a sinusoidal intensity pattern indicated by the periodic line spacings

electron concentration tends to build up in the dimmer regions of the crystal, while the brighter portions of the crystal become depleted of electrons. Thus a dynamic space charge pattern is built up in the crystal by the excess electron concentration in the dim portions of the crystal, and the positive ion concentration in the brighter portions. This space charge pattern alters the refractive index of the crystal through the electro-optic effect. The variation of index of refraction replicates the interference pattern and thus records it.

The hologram that results from recording the sinusoidal illumination pattern is a thick birefringent phase diffraction grating. The hologram is a phase diffraction grating because of the periodic variation in the index of refraction, and is considered a thick diffraction grating because the variation in the index of refraction extends throughout the depth of the hologram.

For the interference pattern just described, the fringes are perpendicular to the applied field. The fringe pattern is recorded in the crystal by net electron movement from brighter regions of the crystal to darker regions, and since the applied field enhances electron movement perpendicular to the fringe pattern, the applied field enhances net electron movement from bright to dark regions. However, as the fringe pattern is rotated with respect to the applied field, the electrons will no longer be moving perpendicular to the fringe pattern. Thus the effect that the applied field has upon net electron movement from bright to dark regions of the crystal is less than for the case of perpendicular fringes, producing a weaker space charge field and index of refraction change in the crystal. In the limit as the fringes become parallel to the applied field, the voltage will

enhance electron movement along regions of constant intensity in the interference pattern, and diffusion due to electron concentration gradients will be the dominate mechanism producing net electron movement from bright to dark regions. In essence, the applied voltage will have minimal influence upon the formation of the space charge field and the space charge field development will be about the same whether the voltage is applied or not. Since it has been reported (Ref. 1) that the diffraction efficiency of a thick diffraction grating formed in BSO with an applied field perpendicular to the fringe pattern can be several orders of magnitude greater than for a thick diffraction grating formed in BSO without an applied field, it can be seen that fringe orientation with respect to the applied field is very important.

There are practical implications of the orientational dependence of fringe storage in BSO crystals. Holograms that use reference and object beams that have large (around 30 degrees or more) angular separations have fringes which tend to be oriented preferentially in one direction. Therefore, when using BSO to record these types of holograms, the fringes will be recorded equally well, since the fringes all tend to be oriented in about the same direction. Other configurations for recording holograms, such as the one used by J.O. White and A. Yariv (Ref. 2), have much smaller angular separations between the reference and the object beams, which produce holograms with fringes that are not as likely to have fringes with a strong preferential orientation. Holograms such as these, with fringes oriented in many directions, will not be uniformly recorded in BSO because the fringe orientation is a factor in how well BSO records the fringes, when a voltage is applied to the crystal. Therefore, it is important

to determine how fringe storage in BSO depends upon the orientation of the fringe with respect to the applied voltage. No study has yet been published that addresses this issue.

One way of determining the orientational dependence of fringe storage in BSO is by measuring diffraction efficiencies of diffraction gratings formed in BSO. A diffraction grating can be produced by recording the interference pattern between two plane waves. Since a diffraction grating has fringes in only one direction, orientational dependence of fringe storage in BSO can be determined by measuring the diffraction efficiencies of diffraction gratings as a function of the angle that the fringes make with the applied field.

The research for this thesis was done at Rome Air Development Center, Hanscom Air Force Base, as part of ongoing research into properties of photorefractives.

B. PROBLEM AND SCOPE

This thesis contains the results of research done to determine how the orientation of a fringe with respect to the applied field in BSO affects how well the fringe gets replicated in the crystal by the index of refraction change induced by the space charge field. This was done by recording thick diffraction gratings in BSO, which have fringes in only one direction, and measuring the diffraction efficiencies. The diffraction gratings were obtained by recording in the crystal a sinusoidal interference pattern produced by interfering two plane waves. Diffraction gratings were recorded and diffraction efficiencies measured for a variety of fringe orientations

ranging from being perpendicular to the applied field to being parallel to the applied field. These measurements were taken for several values of the fringe spacing of the interference pattern, the magnitude of the applied voltage, the modulation coefficient of the sinusoidal interference pattern, and for a wide variety of exposure times. It was decided to vary these parameters to determine if the parameters affect the orientational dependence of fringe storage in BSO. The holograms were made (written) with light having a wavelength of 514.5 nm, and analyzed (read) with light having a wavelength of 632.8 nm. The dimensions of the crystal used in this experiment were 0.8x0.8x0.3 cm.

C. APPROACH

First, for a constant voltage and a constant fringe spacing, the fringes were rotated from 90 to 0 degrees, and diffraction efficiencies and response times were measured at various angles. After these results were analyzed, more diffraction efficiencies and response times were measured the same way, but with different (and constant) voltages and fringe spacings. At the same time, some data was taken with the voltage changed for each angle, in an attempt to verify a model, presented in chapter II, explaining how the effect of the voltage on the space charge growth alters as the angle of the fringes is changed. All the diffraction efficiencies were measured while the voltage remained on.

The diffraction efficiencies were measured by using a read beam that was alternately vertically, horizontally, and randomly polarized, to see if polarization was a significant parameter. The

intensity of the read beam was kept low so that the erase times of the crystal due to the read beam were long relative to the write times of the crystal, to minimize the effect of the read beam erasure upon the diffraction efficiency measurements.

D. ORGANIZATION OF THESIS

In chapter II, the theory supporting this experiment is presented. In chapter III, the equipment used for the experiment is described in detail, and the experimental setup is presented. Chapter IV details the procedure followed in obtaining the data. Results of the experiment are presented and analyzed in chapter V, while practical applications of BSO can be found in chapter VI. Conclusions reached and recommendations for further study can be found in chapter VII.

II. THEORY

A. INTRODUCTION

This chapter describes the basic physical mechanisms behind holographic storage in BSO, since an understanding of these processes is essential for meaningful interpretation of experimental results. First, the physical characteristics of BSO are described, followed by an explanation of the processes involved in holographic storage for the case of a sinusoidal intensity pattern which has fringes perpendicular to the applied voltage, which results in a thick birefringent phase diffraction grating as mentioned in the first chapter. Next is a section describing some of the characteristics of thick phase diffraction gratings. Concluding this chapter is a section which mentions some differences in recording non-perpendicular fringes as compared to recording perpendicular fringes.

B. PHYSICAL CHARACTERISTICS

Bismuth silicon oxide ($Bi_{12}SiO_{20}$) is a wide-band semiconductor with an energy gap of about 3.25ev between the valence and conduction bands at room temperature (Ref. 4). The crystal is optically active, rotating the polarization of light passing through it, and photoconductive. Since a crystal of BSO experiences changes in indices of

refraction when a voltage is placed across it, it is electro-optic. BSO has a dispersive index of refraction as seen in Table I, where values of the index of refraction are tabulated for many wavelengths (Ref. 5). Its absorption coefficient is also quite dispersive as seen in Figure 2 (Ref. 5), ranging from 0.5/cm in the red to 70/cm in the blue. Other characteristic BSO parameters are listed below (Ref. 4):

PARAMETER	BSO
Electro-optic coefficient r_{41}	5×10^{-10} cm V^{-1}
Lifetime-mobility product $\mu\tau$	1.4×10^{-7} cm^2V^{-1}

Energy levels, which result from impurities within the crystal, exist between the valence and conduction bands. These impurities commonly occur in the process of making a crystal such as BSO, and the exact nature of these impurities is not well known at this time. In addition, the crystals can be deliberately doped with impurities. Most crystals produced today are not deliberately doped. Some energy levels occurring from impurities, henceforth called impurity levels, supply electrons for the photorefractive process and also retrap them. Many of the impurity levels are vacant; that is, only a few of them contain electrons which can be used for the photorefractive process. All the electrons that participate in this process originate from these impurity levels, since the band gap is too large for photoexcitation of electrons from the valence band to the conduction band by visible light. Holes can also contribute to the photorefractive process, but since the standard assumption in the field is to neglect their effect, the following development will also neglect their effect.

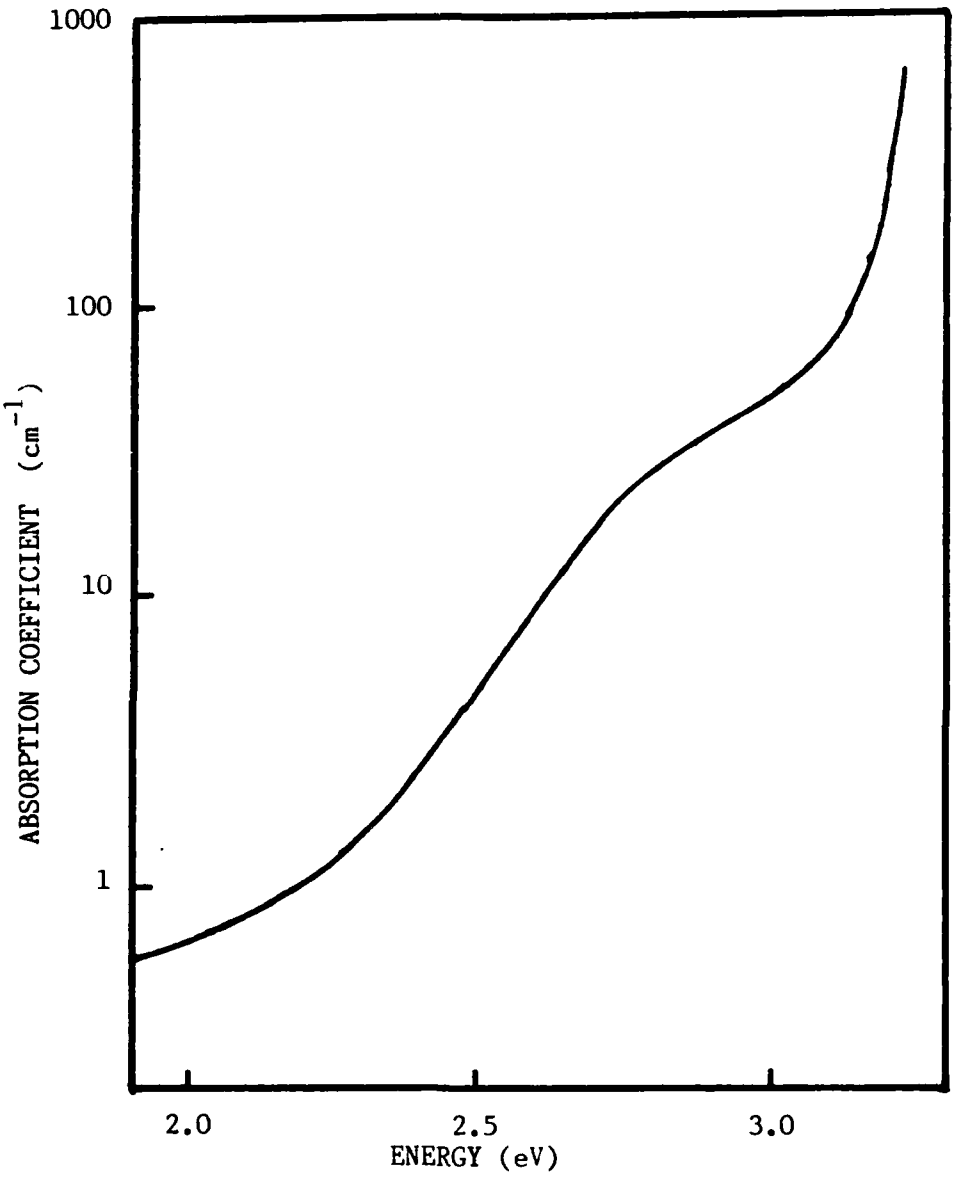

Figure 2. Absorption coefficient of BSO as a function of photon energy

TABLE I

Refractive Index of BSO

Wavelength λ(nm)	$n(\lambda)$
465.8	2.686
472.2	2.674
476.5	2.667
482.5	2.657
488.0	2.650
496.5	2.638
501.7	2.631
514.5	2.615
520.8	2.608
530.9	2.598
568.2	2.566
647.1	2.522
676.4	2.510

C. PHYSICAL PROCESS FOR HOLOGRAPHIC STORAGE

For the following explanation of the physical processes in using BSO for holographic storage, it is assumed that a sinusoidal intensity interference pattern of the form (Figure 3)

$$I(x) = I_0(1 + M\cos Kx) \tag{1}$$

is incident upon the front face of the crystal. Here,

$$I_0 = I_1 + I_2 \tag{2}$$

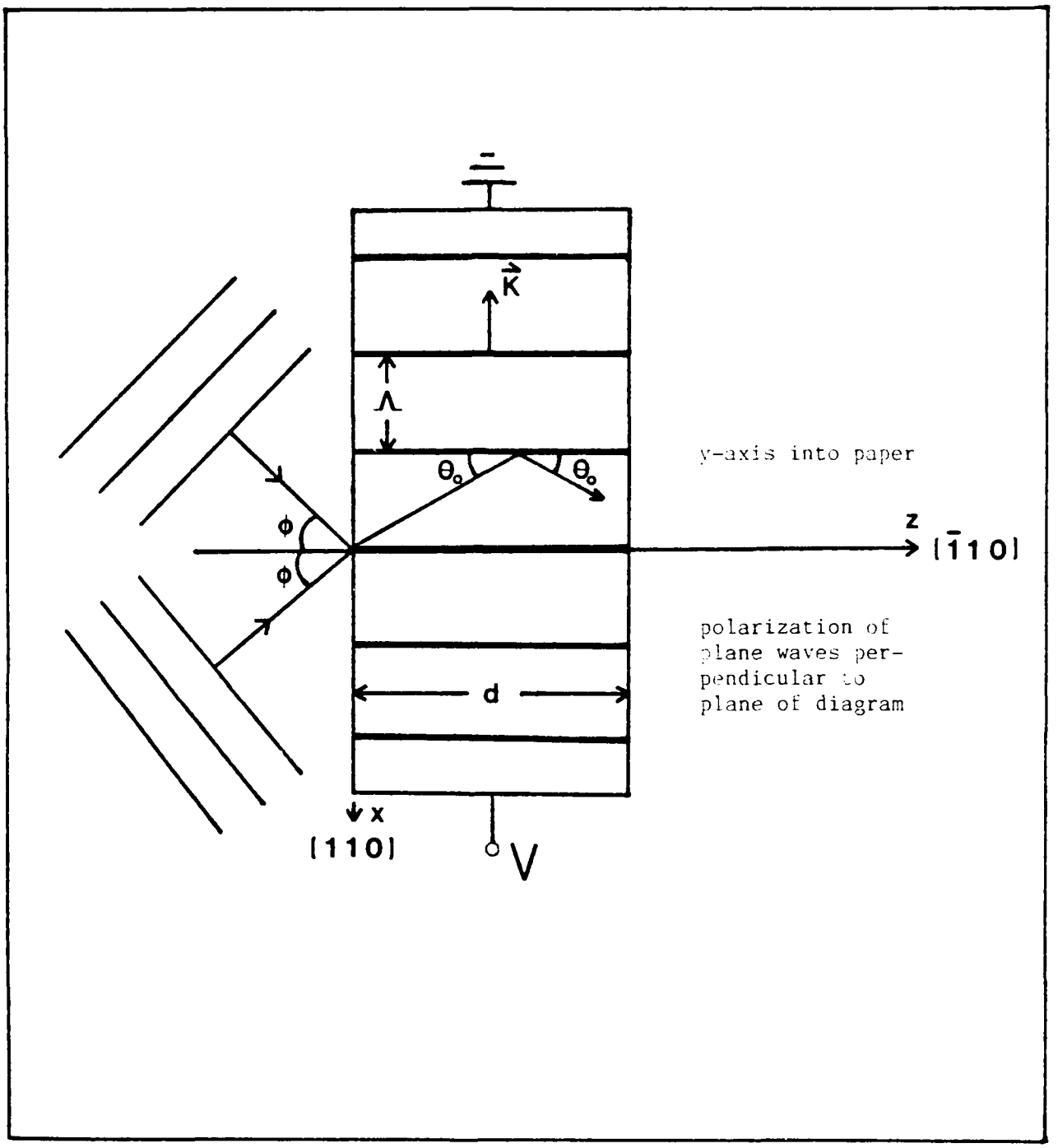

Figure 3. Model of BSO crystal with a sinusoidal intensity pattern and geometry for thick diffraction grating analysis

where I_1 and I_2 are the intensities of the two plane waves forming the pattern; M, the modulation coefficient, and K, the grating vector, are given by

$$M = \frac{2(I_1 I_2)^{\frac{1}{2}}}{I_1 + I_2} \tag{3}$$

$$K = |\vec{K}| = \frac{2\pi}{\Lambda} \tag{4}$$

where Λ is the fringe spacing. This intensity pattern is produced by interfering two uniform plane waves on the front face of the crystal, each making an angle ϕ with the normal to the crystal face. The spacing, Λ, is determined by the angle ϕ according to the relationship

$$\Lambda = \frac{\lambda}{2\sin\phi} \tag{5}$$

where λ is the wavelength in vaccum of the plane wave light. It is assumed that the normals to the plane waves and the normal to the crystal face are coplanar in the x-z plane, thus causing the intensity fringes in the crystal to be perpendicular to the z-axis and parallel to the y-axis. It is also assumed that the only variation of the intensity pattern is in the x-direction.

When this light intensity pattern begins to illuminate the BSO crystal, electrons are excited from the impurity levels into the conduction band, with the excitation rate of these photocarriers proportional to I(x). The electrons now move in the conduction band through both the drift and diffusion processes. In the diffusion process the electrons move to eliminate concentration gradients, while

in the drift process they tend to move in the direction of the applied field. For applied fields in the range under consideration (1 to 5 kilovolts/cm) and for fringe spacings on the order of 1 micron, which is typical for holographic interference patterns, the drift process dominates. These photoexcited electrons eventually become retrapped by the impurity levels, and at the same time more electrons are photoexcited into the conduction band which also become retrapped after moving in the crystal. As this process develops, electrons tend to become trapped in the dimmer regions of the crystal, leaving behind positive ions in the brighter regions of the crystal. A space charge pattern due to these regions of net negative and positive charges develops which opposes the applied field across the crystal. The process reaches steady state when the space charge field balances the applied field, preventing any net movement of electrons in the crystal.

Electrons which have been excited into the conduction band stay there on the average for τ seconds before becoming trapped, where τ is the free carrier lifetime. This lifetime can be related to the average distance the electron drifts before becoming retrapped by the crystal by

$$L_E = \mu\tau E \tag{6}$$

where L_E is called the drift length, μ is the mobility of the electron, and E is the electric field experienced by the electron. A similar expression exists for an electron diffusion length, as discussed in Reference 4.

For short exposure times (the short writing time limit) when the space charge field is very small compared to the applied field, the space charge field is proportional to several parameters as given by (Ref. 6).

$$E_{sc} \propto I_0 Mt \frac{L_E}{\{1 + (KL_E)^2\}^{\frac{1}{2}}} \cos(Kx + \phi_E) \tag{7}$$

where $\phi_E = \tan^{-1} KL_E$. When the space charge field reaches its saturation value, it becomes independent of both the fringe spacing and the drift length and is equal to (Ref. 6).

$$E_{sc} = -\frac{V_0}{d} \{1 - \frac{(1 - M_1^2)^{\frac{1}{2}}}{1 + M_1 \cos Kx}\} \tag{8}$$

where M_1 is an effective modulation ratio and is less than or equal to the modulation coefficient M. The space charge field modifies the index of refraction of the crystal in accordance with the electro-optic effect such that the change in the refractive index is proportional to the space charge field.

Once the illumination I(x) ceases, and assuming that the crystal is then placed in total darkness at room temperature, the space charge field existing in the crystal at the time that I(x) was turned off remains in the crystal for times as long as 30 hours (Ref. 1). The electrons trapped in the impurity levels are eventually reexcited into the conduction band thermally and randomly redistribute, erasing the charge imbalances in the crystal. Light, however, easily excites the electrons into the conduction band since the crystal is photoconductive; therefore, for long storage times, the crystal must be kept

in darkness.

For the information stored (written) in the crystal through the space charge field to be useful, there must be a way to access (read) the information without destroying it. This can be done in several ways. One way is to read the BSO crystal with a wavelength of light that has a correspondingly low absorption coefficient (ideally zero). Another way is to read out the crystal at the same time that the crystal is being written, so that any erasing of the space charge field by the read beam gets repaired by the writing beams. Also, it is convenient to reduce the time and energy necessary to write the space charge field in the crystal. In this case, the wavelength of the write beams is chosen to have a large absorption coefficient, but not too large so that the light will penetrate throughout the crystal, permitting a thick diffraction grating to be formed. If the absorption coefficient is too large, the light will be absorbed only on the surface of the crystal. Currently, several experiments have used the argon green laser line (wavelength of 514.5nm) for the write beams, and have used helium neon laser light (wavelength of 632.8nm) for the read beam. Many times, when the reading of the crystal is done simultaneously with the writing of the crystal, the read beam is the same wavelength as the write beams, with the read beam counterpropagating along one of the write beam paths (the so-called degenerate four-wave mixing configuration). This configuration is generally used for applications of BSO to phase conjugation.

To erase the space charge field in the crystal, a uniform beam of light illuminates the crystal with the write beams turned off. The erase beam can be a separate light beam, or can be one of

the write beams when the other write beam is blocked. The applied voltage usually remains on during the erase cycle.

D. THICK DIFFRACTION GRATINGS

In the example above, it was stated that in the short writing time limit, the space charge field set up in the BSO crystal was proportional to the intensity I(x) and thus sinusoidal. The variation in the index of refraction is also sinusoidal which produces a thick diffraction grating since the variation in the index of refraction extends throughout the depth of the crystal. Even when the space charge field is non-sinusoidal, it is still periodic, and thus still produces a thick diffraction grating. Thick diffraction gratings possess a number of important features such as wavelength and angular selectivities, and the capability for high diffraction efficiencies, which thin diffraction gratings do not possess. However, an absorption diffraction grating also produces additional light loss.

H. Kogelnik (Ref. 7) developed a theory for thick sinusoidal diffraction gratings using a coupled wave analysis which detailed a number of properties of thick diffraction gratings, including analytical expressions for angular and wavelength sensitivities, and diffraction efficiencies. A lossy phase diffraction grating has a diffraction efficiency given by

$$N = \{\exp(\frac{-\alpha d}{\cos\theta_0})\}\{\sin^2(\frac{\pi n n' d}{2\lambda \cos\theta_0})\} \qquad (9)$$

where α is the intensity absorption coefficient for the read beam,

n is the unmodulated index of refraction of the crystal, n' is the peak to peak change in the index of refraction, d is the thickness of the crystal, λ' is the read beam wavelength of light in vacuum, and θ_0 is the Bragg angle inside of the hologram as given by

$$2\Lambda\sin\theta_0 = \frac{\lambda'}{n} \tag{10}$$

Absorption in the crystal precludes the possibility of achieving a diffraction efficiency of 100%; to utilize the thick grating efficiency enhancement, the loss from absorption must be less than the improvement from the additional diffraction by the thickness.

The levels of constant n in the crystal, which are parallel to the z-axis in Figure 3, act as Bragg planes, giving the crystal its properties of angular and wavelength sensitivities. For a given wavelength, the angle of incidence inside the medium needed for maximum diffraction efficiency is given by equation (10). As the angle varies from θ_0, the diffraction efficiency will fall off and eventually reach zero. The same explanation holds for wavelength sensitivity for a given angle of incidence. An approximation for the angular selectivity for this type of thick grating is

$$\Delta\theta_0 \simeq \frac{\Lambda}{d} \tag{11}$$

and a similar approximation exists for the wavelength selectivity

$$\frac{\Delta\lambda'}{\lambda'} \simeq \frac{\Lambda\cot\theta_0}{d} \tag{12}$$

where a change in angle of $\Delta\theta_0$ from θ_0 or a change in wavelength of

$\Delta\lambda'$ from λ' leads to a diffraction efficiency of zero. Also, if the diffraction grating is written with one wavelength of light, and is read with another, the angle of the read beam must be different from that of the write beam to satisfy the Bragg condition as given in equation (10).

If the variation in the index of refraction of the crystal is not sinusoidal, but still periodic (as for the saturation space charge field), diffraction also occurs for Bragg angles larger than the fundamental angle θ_0. Expressions for the diffraction efficiencies for the various orders become much more complicated, and can be found in Reference 8.

Kogelnik's theory assumes that the grating is uniform throughout the depth of the medium, the polarization of the read beam is perpendicular to the plane of incidence, and the medium is non-birefringent. However, gratings formed in BSO are not uniform throughout the crystal due to absorption. BSO is also optically active, with the activity wavelength dependent, and is birefringent when a voltage is applied. The birefringent nature of diffraction gratings stored in BSO is especially critical to account for when applying Kogelnik's theory. Kogelnik assumed for his theory given by equation (9) that the diffraction grating only has one propagation mode, which is parallel to the planes of constant index of refraction, and that the light beam being diffracted is polarized along the propagation mode. For birefringent gratings, two propagation modes exist, and in general neither of them are parallel to the planes of constant index of refraction. Therefore, to apply Kogelnik's theory to birefringent diffraction gratings, his theory must be extended to include the effects of a light beam with

arbitrary polarization being diffracted. Because the two propagation modes are orthogonal to each other, light propagating along each mode can be considered to be diffracted independently. In the results chapter of this thesis, Kogelnik's theory is assumed to hold for arbitrary polarization of the read beam, and light propagating along one mode is considered to be diffracted independently of light propagating along the other mode. In the literature, no one has extended Kogelnik's work to birefringent diffraction gratings. This is an area which needs to be addressed.

E. NON-PERPENDICULAR FRINGES

When the fringes are not perpendicular to the applied voltage, the theory presented above needs to be modified in at least two areas. The first modification is needed due to the change in the effect that the applied field has upon the space charge field formation, and the second modification is needed because of the effect that the direction and magnitude of the space charge field has upon the changes in the index of refraction of the crystal.

When the fringes are not perpendicular to the applied voltage, the photoexcited electrons no longer move perpendicular to the fringes. As the fringes become parallel to the applied field, the applied voltage has essentially no effect upon the space charge field formation. The falloff of the effect that the applied field has upon the space charge field formation can be explained (Ref. 9) by referring to Figure 4. Figure 4(a) shows the envelope of electron migration along drift length AC for the case of fringes perpendicular to the applied

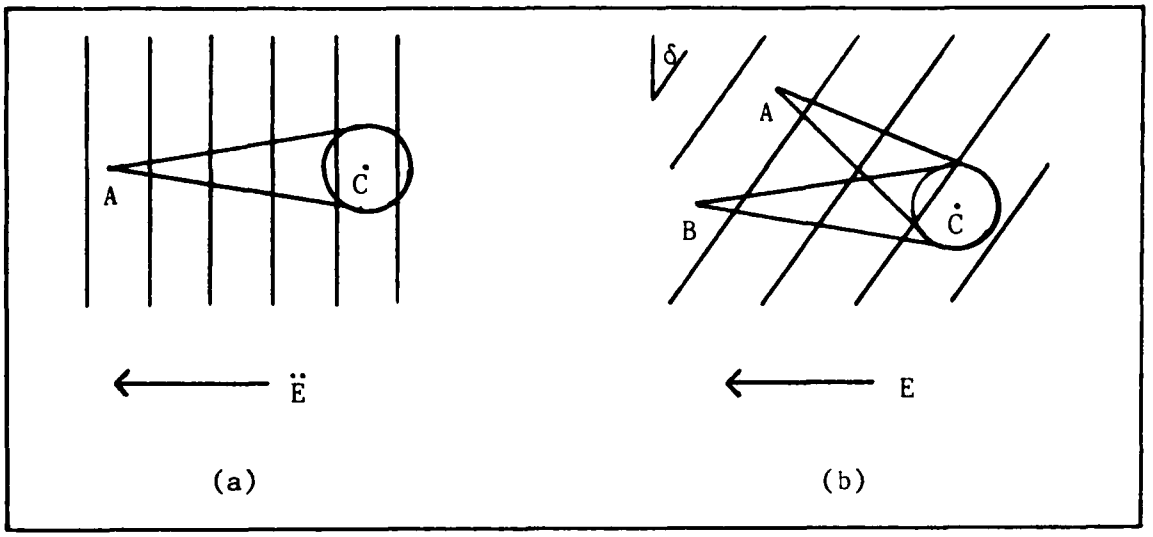

Figure 4. Electron migration in BSO for a sinusoidal intensity pattern: (a) perpendicular to applied field, (b) non-perpendicular to applied field

field. Figure 4(b) shows the envelope of electron migration along drift length BC for the case of non-perpendicular fringes. Since the illumination is uniform parallel to the fringes, the space charge built up in the short write time limit (when the applied field is much greater than the space charge field) along drift length BC due to E is identical to that built up by $\ddot{E}$ along drift length AC. Since AC is equal to BC multiplied by the cosine of δ, it appears that effective drift length of the electron for non-perpendicular fringes is proportional to the cosine of the angle between the fringes and the applied field. Since the drift length is proportional to the magnitude of the applied field for short write times, it appears that the effect of the applied field in the material falls off as the cosine of δ. Another way to express this effect is to say that only the

component of the applied field perpendicular to the fringe pattern enhances the space charge pattern formation.

The second point that needs to be considered for non-perpendicular fringes is the dependence of the index of refraction of the crystal upon the magnitude and direction of the field inside. For a birefringent crystal, there are two independent and orthogonal propagation modes which depend upon the direction of the incident light wave k-vector, and both of these modes are orthogonal to the k-vector. The propagation modes are polarization dependent; that is, light incident upon a birefringent crystal with a given polarization excites each of the two modes by an amount dependent upon the magnitude of the component of the polarization in each mode. For example, if the direction of polarization of the incident light beam is in the direction of only one of the modes, it will excite only that mode. If the direction of polarization of the light beam is 45 degrees to each mode, then each mode will be excited equally. Each of these propagation modes has an index of refraction associated with it, and in general the two indices of refraction are different.

While BSO is isotropic without an applied voltage, it becomes birefringent with an applied voltage. The direction of the propagation modes and the magnitudes of the index of refraction changes depend upon the magnitude and direction of the local internal field inside the crystal, as well as the direction of the incident light beam. For a theoretical development describing these effects, see Reference 10. It is sufficient to say here that in a paper written by M. P. Petrov and A. V. Khomenko (Ref. 11), closed form solutions were given to find both the direction of the propagation modes and

the magnitudes of the index of refraction changes for each of the modes. However, for fringes not perpendicular to the applied voltage, the development of the space charge field inside the crystal is highly complex. The detailed growth of the index of refraction changes in the crystal would require a careful computer study.

III. EQUIPMENT

A. INTRODUCTION

The equipment used for this experiment is shown in a block diagram form in Figure 5, and Figure 6 is a photograph of the equipment setup. The output beam from the argon laser (wavelength of 514.5 nm) is spatially filtered and expanded, collimated, and then split into two beams which impinge upon the BSO crystal, producing a sinusoidal interference pattern. This interference pattern is recorded in the BSO crystal, producing a thick diffraction grating which diffracts part of the read beam from the helium neon laser (wavelength of 632.8 nm). The diffracted beam impinges upon the input to the photomultiplier (PM) tube, and the output of the PM tube is measured on the oscilloscope. It is necessary to mount the equipment upon an air table to help isolate the experiment from vibrations.

The experimental setup will be described in the following four sections: write beam equipment, crystal holder, read beam equipment, and detection equipment.

B. WRITE BEAM EQUIPMENT

The apparatus used to produce the write beams is shown in block diagram form in Figure 7. The argon laser is a Spectra Physics model

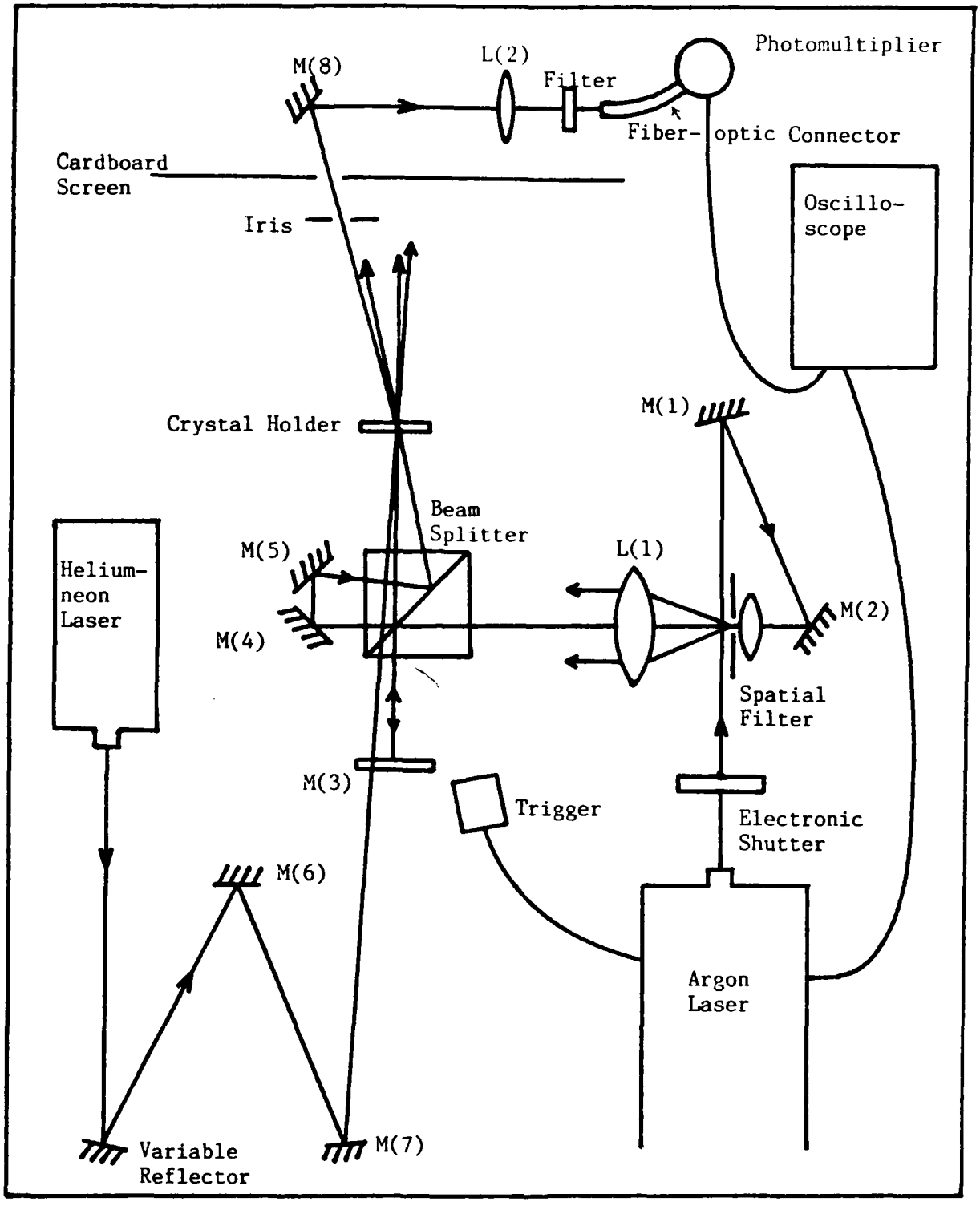

Figure 5. Block form diagram of experimental setup

Figure 6. Photograph of experimental setup

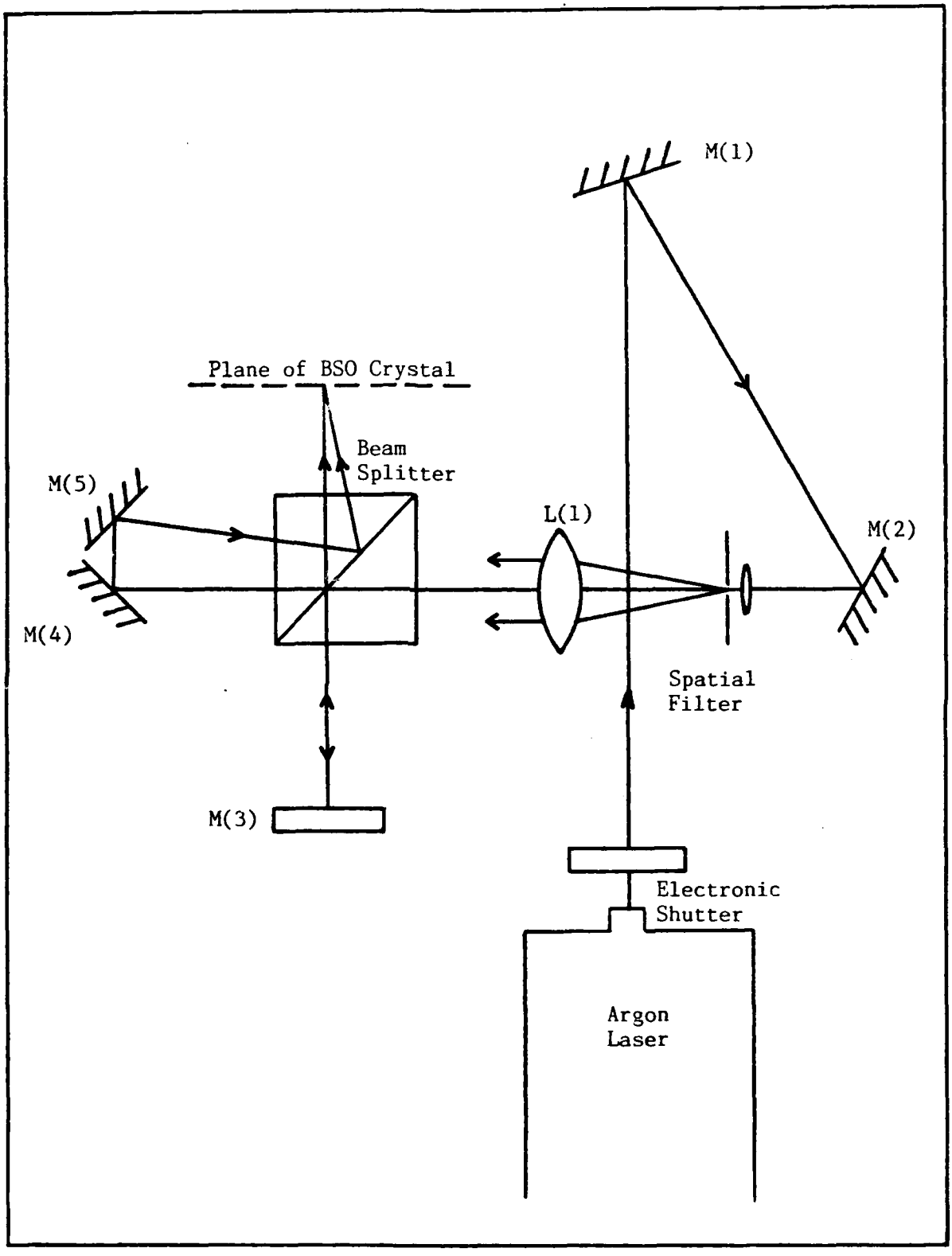

Figure 7. Write beam equipment

165, whose output passes through an electronic shutter which can be set to stay open for any length of time from 0 to 10 seconds. The laser beam, which is vertically polarized, reflects off of mirrors M(1) and M(2) which permit horizontal and vertical adjustments of the laser beam. Then the beam passes through a Jodon spatial filter which has a 20X microscope objective and a 10 micron pinhole. The output from the spatial filter is collimated by the lens L(1).

The light beam now enters an interferometer formed by the beam splitter cube and the mirrors M(3), M(4), and M(5). The beam splitter reflects 50% and transmits 50% of the light beam. Light reflected from mirrors M(4) and M(5) re-enters the beam splitter and is reflected towards the plane of the BSO crystal at an angle different from that of the light reflected from mirror M(3), producing the desired sinusoidal intensity pattern. This angle can be varied by changing the positions of M(4) and M(5), which in turn varies the spatial frequency of the pattern.

Several considerations need to be mentioned now. The interferometer setup used to create the two plane waves needed to produce a sinusoidal intensity pattern on the BSO crystal was chosen after analyzing several other possible setups, because the interferometer setup produced the most stable interference pattern. Also, the laser beam has a gaussian intensity profile instead of the desired uniform intensity profile, so the light beam was expanded to a four centimeter diameter, and the eight millimeter square BSO crystal was illuminated by just the center of the light beams, where the intensity profile is the most uniform. Finally, while mirrors M(1), M(2), M(4), and M(5) are 100% reflecting front surface mirrors, mirror M(3) is a

dielectric coated mirror with a reflectance coefficient of 20%. Mirror M(3) was chosen to be coated to allow the read beam to be able to transmit through it, while allowing the two write beams to have different intensities, resulting in a modulation coefficient M of less than unity. As seen in equation (8), very small values of M produce a sinusoidal steady state space charge pattern in the crystal. Even if M is too large to produce a sinusoidal steady state pattern, smaller values of M allow the buildup of the space charge pattern to remain sinusoidal longer into the write cycle.

C. CRYSTAL HOLDER

The BSO crystal is mounted in a rotating holder that is calibrated in degrees, which is mounted upon an NCR model 39 tilt table that permits both horizontal and vertical tilt adjustments. A picture of the holder is shown in Figure 8. The high voltage leads, held against the crystal sides by plastic bolts, are connected to the crystal using silver paste to ensure a good electrical connection. A Power Designs Pacific high voltage (up to 5kV) power supply provides the voltage for the crystal.

D. READ BEAM EQUIPMENT

In Figure 9, the apparatus used to generate and direct the read beam onto the BSO crystal to measure diffraction efficiencies is shown in block diagram form. This read beam, supplied by an unpolarized Spectra Physics model 132 helium neon laser, is reflected

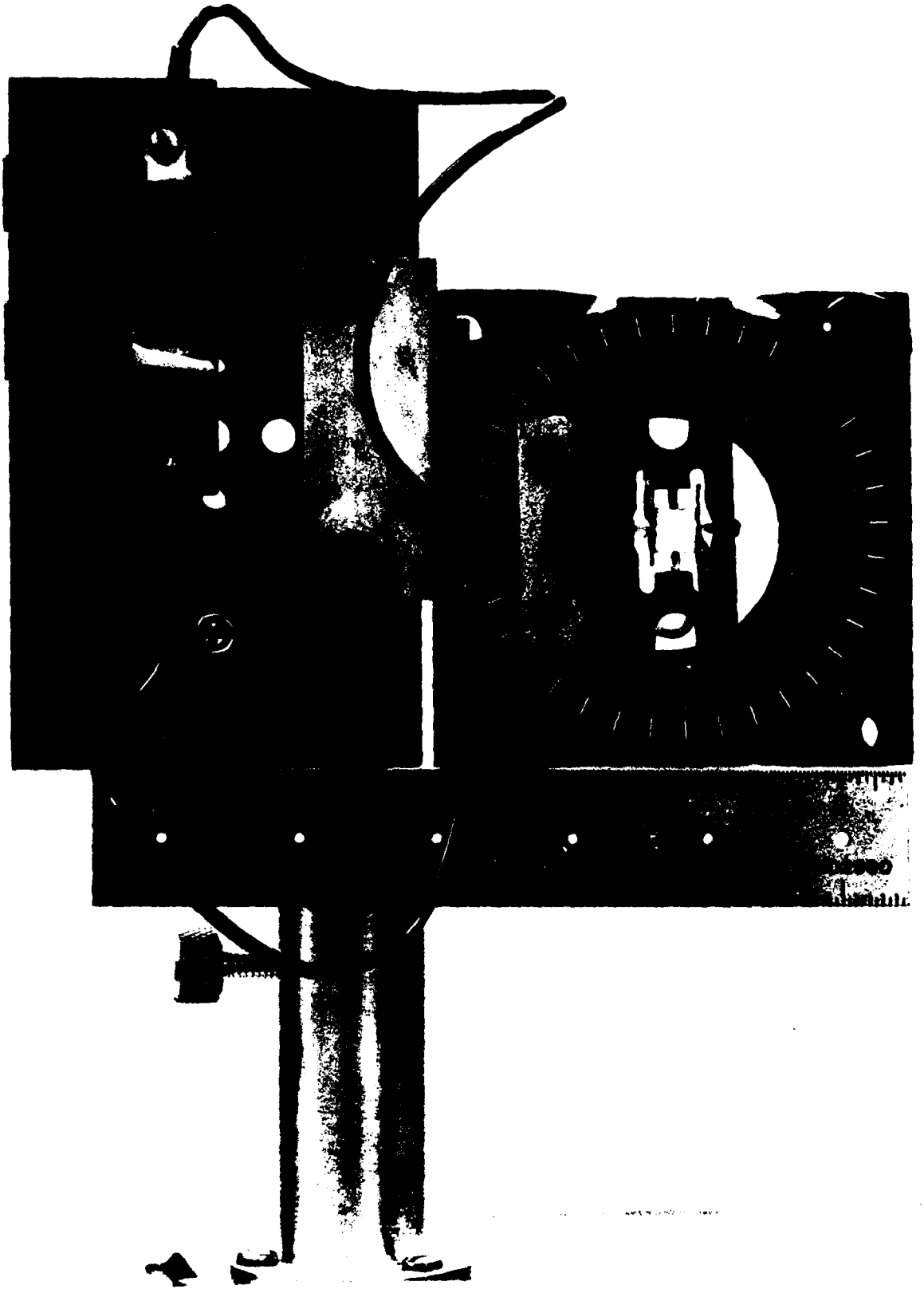

Figure 8. Photograph of BSO and crystal holder

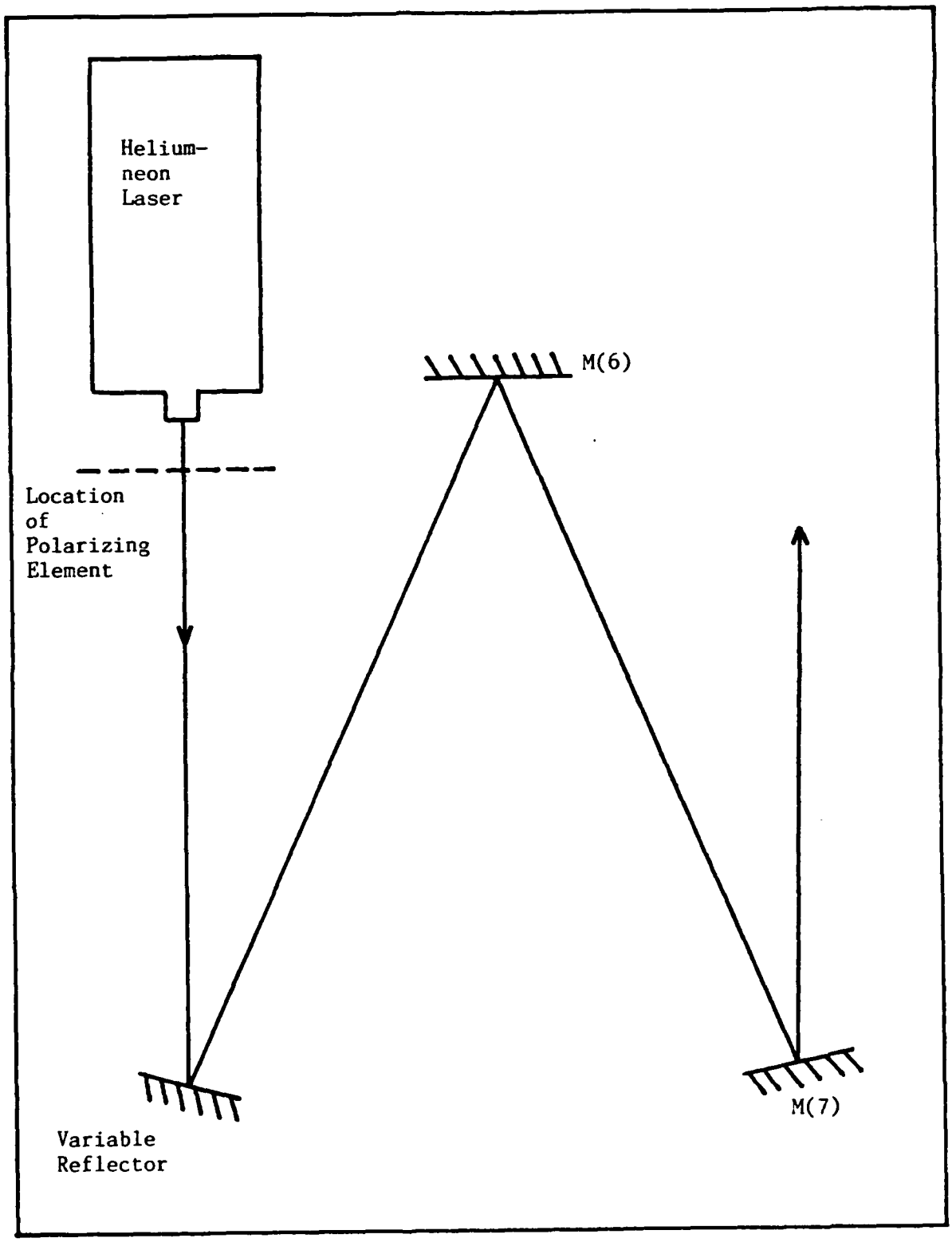

Figure 9. Read beam equipment

by a variable reflector, which allows the power of the read beam to be adjustable. Mirrors M(6) and M(7), which provide vertical and horizontal adjustment of the read beam, are used to align the beam to the appropriate fundamental Bragg angle of the thick diffraction grating. This angle is different from the angle of the write beams, since the Bragg angle depends upon the wavelength of the light beam. As mentioned earlier, the read beam passes through mirror M(3), since the Bragg angle for the read beam is almost the same as the angle of the write beams.

For some of the measurements taken, the read beam was polarized by placing a rotating polarizing element between the laser and the variable reflector.

E. DETECTION EQUIPMENT

The equipment used to detect and measure the strength of the diffracted beam is shown in block diagram form in Figure 10. The iris, the cardboard screen, and black cloths are used to block out the write beams, and pass the diffracted component of the read beam, which is reflected by mirror M(8) and focused by lens L(2) onto a fiber optic coupler to an Oriel 7062 photomultiplier tube. The output from this PM tube, which is powered by a Fluke model 412b high voltage power supply, is displayed upon the A vertical input channel of a Tektronix model 7854 digital oscilloscope through a model 7A22 differential amplifier. The time base for the oscilloscope is a model 71392A dual time base.

To help block out the green light from the write beams in the

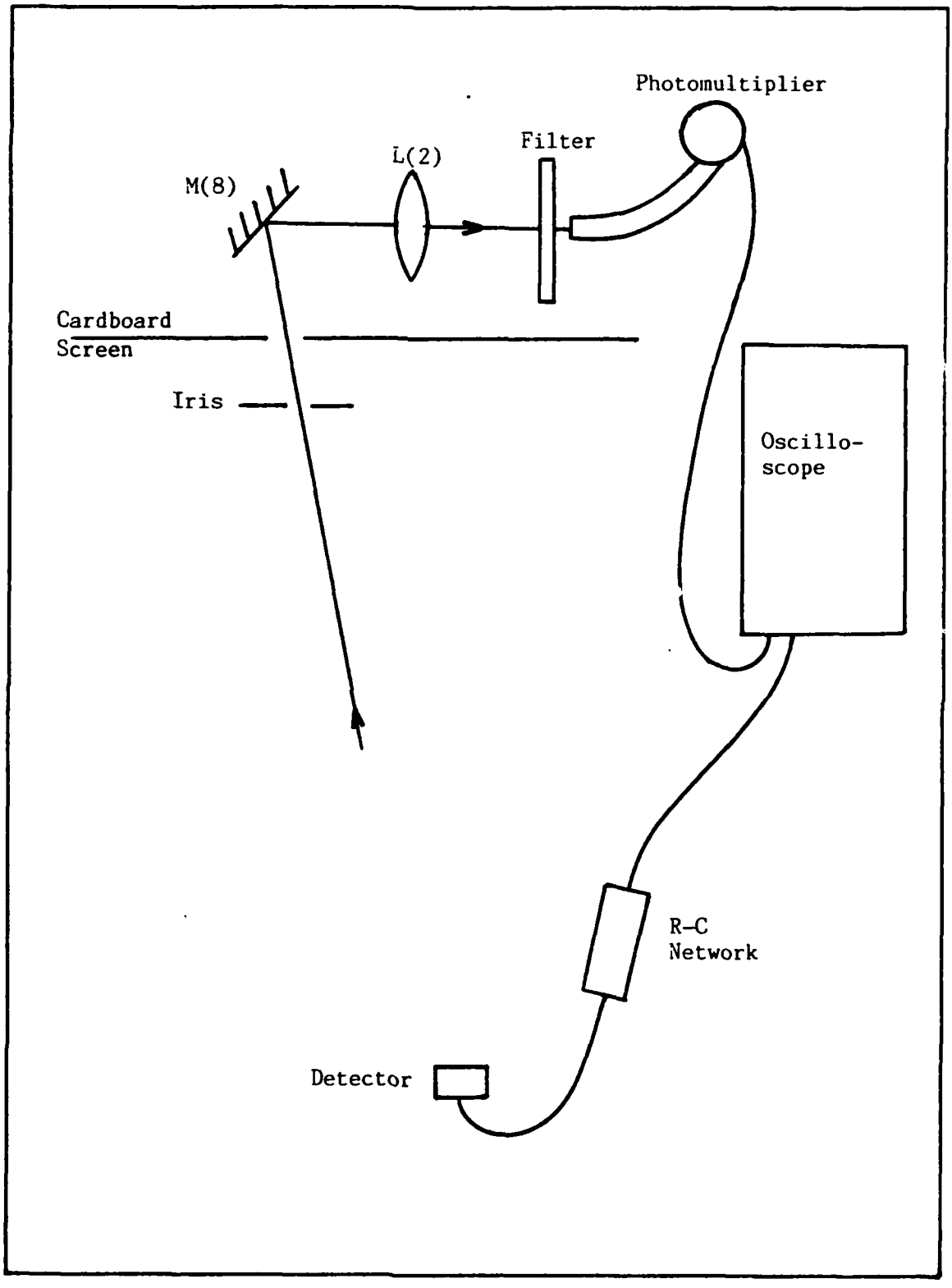

Figure 10. Detection equipment

detector setup, a filter which transmits only red light is placed in the diffracted beam path directly in front of the fiber optic coupler. Black cloths are draped over the cardboard screen, M(8), L(2), the filter, and the PM tube with the fiber optic coupler, leaving only the hole in the cardboard screen as a place where light can enter the detection setup.

Light from the write beams is used to trigger the oscilloscope, allowing the very beginning of the diffracted beam traces to be displayed. In order to keep the trigger signal constant and independent of the angle of the BSO crystal, the photodetector is positioned so that it is illuminated by a write beam reflection from the beam splitter cube, which does not change in intensity or position when the crystal is rotated. The output of the photodetector is passed through a simple RC network to change the dc steady state signal from the photodetector to a pulsed output. The output of the RC network connects to the B vertical input channel of the oscilloscope by a Tektronix model 7A16A amplifier. By connecting the trigger to a vertical input channel instead of the external trigger input on the oscilloscope, the trigger trace can be monitored to ensure the triggering signal remains constant.

A laser power meter is used to measure the power of the write, read, and diffracted beams. The power meter is a NCR model 820, which is calibrated for laser light of wavelengths 514.5 nm, 632.8 nm, and 488.8 nm. The meter can measure powers ranging from 5 nW to 100 mW.

IV. PROCEDURE

A. INTRODUCTION

The procedure followed during the course of the experimental work will be explained in detail in this chapter. The first section will describe the alignment procedures, and the second section will explain how the data was obtained.

B. ALIGNMENT

The first step in aligning the experimental apparatus is to adjust the angle separating the two write beams to achieve the desired fringe spacing Λ. Only mirrors M(4) and M(5) are moved to achieve different fringe spacings, and both write beams are kept parallel to the table surface, causing the fringes to be perpendicular to the surface. The write beam that is reflected by M(3) is adjusted to re-enter the beam splitter cube back along the original beam path for all fringe spacings. For the setup used in this experiment, the write beam reflected by M(3) was adjusted to enter the beam splitter cube slightly off-normal to avoid an interference pattern in the plane of the BSO crystal caused by spurious reflections from the beam splitter cube faces. Then, to adjust the angle between the two write beams, mirrors M(4) and M(5) are moved relative to each other and the beam

splitter cube to adjust the angle of the write beam re-entering the cube and thus altering the angle between the two write beams.

To determine the angle existing between the write beams, a piece of cardboard is placed at a predetermined distance behind the BSO crystal, and the distance between the two light beams illuminating the crystal is measured. Using simple trigonometry, the angle can be determined. By marking the distance required between the two write beams for a given distance behind the BSO crystal for a desired angular separation (and thus a desired fringe spacing) with two lines on the piece of cardboard, mirror adjustment becomes quite simple. The piece of cardboard is positioned such that one of the lines is aligned with the write beam reflected by M(3), and mirrors M(4) and M(5) are re-positioned to align the other write beam onto the second line. Of course, at the same time, both beams are positioned to illuminate the crystal with the center of each write beam. Also, the optical path lengths of the two arms of the interferometer must be very nearly equal in length. The mirrors were positioned to produce an optical path length difference of less than a centimeter, since the measurements were not sensitive to small (a few millimeters) translation of one of mirrors. Either mirror M(3) or mirrors M(4) and M(5) can be moved to equalize the optical path lengths.

Once the write beams are properly aligned, the crystal needs to be aligned to assure that the write beams and the normal to the face of the crystal are all coplanar, and that both write beams strike the crystal at equal angles from the normal to the crystal face. This is done by blocking the write beam that normally reflects off of M(4) with a piece of paper or cardboard between the beam splitter

cube and M(4), and adjusting the crystal mount until the portion of the other write beam that is reflected by the front face of the BSO crystal back-reflects along the blocked write beam's path.

The fundamental Bragg angle for the read beam is slightly larger than the angle of the write beams since the read beam wavelength is larger than the write beam wavelength. To align the read beam, the piece of cardboard with two marks used to align the write beams is marked with a third line that is at the proper distance to give the correct Bragg angle for the read beam. Mirrors M(6) and M(7) are adjusted until the read beam, after passing through the BSO crystal, strikes the third line on the cardboard screen.

Once the write beams, the BSO crystal, and the read beam are properly adjusted, the cardboard used for adjustment is moved out of the way, and the voltage across the crystal is turned on. Usually, a strong diffracted beam is seen, and then the read beam is adjusted in small amounts to maximize the diffracted beam. The diffracted beam is then passed through the hole in the cardboard screen, reflected by M(8), focused down by L(2), passed through the filter, and positioned on the end of the fiber optic connector which is placed in the focal plane of L(2). After shielding the detector setup with the black cloths, the power supply for the photomultiplier is turned on, with the output from the PM displayed upon the oscilloscope. Then the read beam is adjusted by adjusting mirrors M(6) and M(7) until the diffracted beam power is maximized.

After the read beam has been adjusted to maximize the diffracted beam power, it is necessary to determine how quickly the read beam erases gratings in the crystal after the write beams are turned off.

This is done by writing a grating into the crystal until steady state has been reached, then blocking the write beams with the electronic shutter and seeing how quickly the diffracted beam power as seen on the oscilloscope goes to zero. The variable reflector for the read beam is adjusted until the erase time of the read beam is much longer than the write times of the write beams. Ideally, the power of the read beam may be adjusted until the erase time is at least an order of magnitude longer than the longest write time. However, a less intense read beam (resulting in a longer erase time) yields a weaker diffracted beam, producing increased noise on the oscilloscope traces. A compromise between the erase time of the read beam and the power of the diffracted beam must be reached when adjusting the power of the read beam.

C. DATA GATHERING PROCEDURES

Data obtained for this experiment was gathered during processes called data runs. To prepare for a data run, the write beams are adjusted to produce the desired fringe spacing, and this fringe spacing stays the same for the entire data run. The relative intensities of the two write beams may be altered to produce the desired value of the modulation coefficient by placing a neutral density filter between M(3) and the beam splitter cube. This modulation coefficient also stays the same for the data run. Then the photodetector used to trigger the scope is positioned to be triggered by a stray write beam reflection. Finally, the BSO crystal is rotated to all the desired angles, starting with the fringes perpendicular to the applied

field, and ending with the fringes parallel to the applied field. Every time the crystal is rotated, alignment needs to be done, and the necessary data is then obtained. Since the procedure is the same for any angle of the BSO crystal, data gathering procedures will be described for only one angle.

First, the BSO crystal is rotated to the desired angle. This is done by rotating the crystal until the applied field is perpendicular to the fringes, and noting the degree marking on the crystal holder. All angles used for data taking should be referenced to this value. Then, after rotating the crystal to the desired angle, the back-reflection of the front face of the crystal is aligned as described earlier. At this time, it should be determined if the read beam will be polarized or unpolarized for the data taking, and if polarized, what polarization is desired. A polarizer should be inserted in the read beam path between the helium-neon laser and the first mirror the read beam encounters if a polarized beam is desired, with the polarizer oriented correctly for the desired polarization. Since the helium-neon laser is unpolarized, for unpolarized data nothing needs to be inserted in the beam path. Once the read beam is polarized properly, the read beam is adjusted to maximize the diffracted beam power using previously mentioned procedures, and the power of the read beam is adjusted to obtain a long erase time. If data needs to be taken for several polarization states of the read beam for one angle of the crystal, the alignment of the read beam should be tested for each polarization.

Once the read beam is polarized properly and adjusted for maximum diffracted beam power and long erase times, the value of the applied voltage is set on the power supply to the desired value. Since no alignment needs to be done for different values of the applied voltage, data should be taken for all the necessary voltages without adjusting any other parameter such as read beam polarization or crystal angle.

Now, having positioned the BSO crystal to the correct angle, adjusted the read beam for the desired polarization, and chosen the value of the applied voltage, data on write times can be obtained by recording write traces with the oscilloscope. The oscilloscope can store and average up to 1000 traces; for this experiment, the oscilloscope was set to average 10 write traces. The averaging was done to help reduce the noise in the write traces. Before writing a grating, the crystal is erased by blocking one write beam and allowing the uniform illumination from the other write beam to eliminate any previously stored interference pattern. Then the electronic shutter is shut off, cutting off the write beams from the crystal. The read beam is never blocked. After about a 2 second delay to allow air currents and table vibrations to die out, the electronic shutter is opened, allowing the write beams to impinge upon the crystal while the rise time of the diffracted beam (the write trace) is stored by the oscilloscope. The crystal is then erased and written again, until the required number of write traces have been averaged. The resultant averaged trace is displayed upon the oscilloscope, and values of the diffracted beam as a function of the write time can be obtained.

The oscilloscope does not display the actual power of the

diffracted beam, only the relative magnitude. To calibrate the photomultiplier, the laser power meter is used to measure the power of the diffracted beam, and this value is compared to the value seen upon the oscilloscope. Now all oscilloscope readings can be converted to actual power readings for the diffracted beam. By measuring the power of the read beam before it impinges upon the crystal, absolute diffraction efficiencies can also be obtained.

V. RESULTS

A. INTRODUCTION

Data obtained for diffraction efficiencies of thick holograms in a BSO crystal will be presented and analyzed in this chapter. Problems encountered with the steady state diffraction efficiencies are discussed in section B. Theoretical predictions for diffraction efficiencies of diffraction gratings made with short exposure times can be found in section C, and experimental diffraction efficiency data can be found in section D.

B. STEADY STATE DIFFRACTION EFFICIENCIES

Significant fluctuations in the steady state diffraction efficiencies for thick holograms in BSO were encountered during the experimental work. These fluctuations ranged up to a factor of 2 or more from the average steady state values. The problem seemed to be due to vibrations and air currents in the room. In particular, for this experiment, a water pump for the power supply of the argon laser was present near to the experimental setup. This pump was mounted to the wall of the room in which the experimental work was done, and the pump vibrated quite a bit.

No enclosure was used to shield the experiment from air

vibrations, yet air vibrations have been shown to be a significant problem, especially for long exposure times (Ref. 12). For exposure times of 100 ms or less, an enclosure only provides a few percent better fringe stability over a non-enclosed experiment. However, for a write time of 1 second or more, the efficiency of a non-enclosed holographic setup is down to 50 percent of an enclosed setup. Remembering that the air currents fluctuate with time, it can be seen that large fluctuations in the steady state diffraction efficiencies are to be expected for a non-enclosed holographic setup. However, for exposure times of 100 ms or less, air currents should have much less of an effect upon diffraction efficiency measurements.

The experiment was originally conducted upon an air table that had an enclosure. The argon laser discharge tube cracked, forcing a move to an air table that did not have an enclosure, and time constraints did not allow for an enclosure to be built upon the new air table. To make as accurate as possible the steady state diffraction efficiency measurements, the steady state traces upon the oscilloscope were observed for a minute or more, and an average value was decided upon. Most of the fluctuations were 10 to 20 percent of the average value, with occasional fluctuations that were much larger. These larger fluctuations were discounted, and the error bars associated with the steady state diffraction efficiency measurements only reflect the 10 to 20 percent variations.

C. THEORETICAL PREDICTIONS

Diffraction efficiencies of thick phase diffraction gratings

formed in BSO crystals were obtained for several values of the modulation coefficient, fringe spacing, applied voltage, fringe angle, and read beam polarization. To determine the quality of the data, it must be compared to theoretical predictions. Equation (7) gives the functional dependence of the space charge field upon these parameters for fringes perpendicular to the applied field and for short exposure (write) times. Since the change in the index of refraction is proportional to the local electric field in the crystal, the diffraction efficiency of a BSO diffraction grating is proportional to the square of the space charge field for very small changes in the index of refraction, assuming only one propagation mode in the crystal is excited. If both propagation modes are excited, the diffraction efficiency for light propagating in each mode is proportional to the magnitude of the space charge field. However, for fringes perpendicular to the applied field and for the crystallographic orientation of the sample used in this experiment, both propagation modes have identical absolute values for the index of refraction changes. This implies that Kogelnik's theory holds for any polarization of the read beam for this configuration, since each propagation mode diffracts incident intensity identically. Therefore, the diffraction efficiencies for fringes that are 90 degrees to the applied field should be proportional to the square of the space charge field for short write times. The following paragraphs will outline theoretical predicted changes in the diffraction efficiency as the applied voltage, fringe spacing, and modulation coefficient are varied. These predicted changes are assumed to be independent of the polarization of the read beam, and will be used to compare data to theory for all read beam polarizations.

Data in this experiment was obtained for both a modulation coefficient of 0.82 and 0.45. Since the lower modulation coefficient was obtained by decreasing the intensity of one of the write beams, the intensity I_0 (see equation (2)) is also decreased by a factor of 0.84. Then, by using these values in equation (7), it can be seen that the short write time theory predicts a falloff in the diffraction efficiency by a factor of 0.21 as the modulation coefficient is decreased from 0.82 to 0.45 with all other parameters held constant.

Another parameter that was varied was the fringe spacing. For an applied voltage of 5kV, with other parameters held constant, the diffraction efficiency for a fringe spacing of 3 microns should be a factor of 0.36 lower than for a fringe spacing of 5 microns. For an applied voltage of 1kV, with other parameters held constant, the diffraction efficiency for a fringe spacing of 3 microns should be a factor of 0.40 lower than for a fringe spacing of 5 microns.

The last parameter for which theoretical predictions will be made is for values of the applied voltage. For a fringe spacing of 5 microns, there should be no change in the diffraction efficiency as the applied voltage decreases from 5kV to 3kV, but as the applied voltage changes from either 5kV or 3kV to 1kV, the diffraction efficiency should also decrease by a factor of 0.85. For a fringe spacing of 3 microns, there again should be no change in the diffraction efficiency as the applied voltage decreases from 5kV to 3kV, but as the applied voltage changes from either 5kV or 3kV to 1kV, the diffraction efficiency should also decrease by a factor of 0.93.

D. WRITE TIME DATA

UNPOLARIZED READ BEAM. The helium-neon laser used to supply a read beam to be diffracted by diffraction gratings in BSO was unpolarized, but had 1.8 times as much power in the horizontal polarization as in the vertical polarization. The experimental data for the unpolarized read beam and constant applied voltage is shown in Figures 11, 12, 13, 14, and 15. Figure 11 is a linear-linear plot of diffraction efficiency versus time for several fringe angles and for an applied voltage of 3 kilovolts, a fringe spacing of 5 microns, and a modulation coefficient of 0.82. Each curve in Figure 11 shows a typical time development of diffraction efficiency as displayed upon the oscilloscope. This figure is given to show the reader what the raw data looked like that was obtained during the experiment. Figures 12, 13, 14, and 15 are semi-log plots of diffraction efficiency versus fringe angle for many write times. Data in Figure 12 is for an applied voltage of 5 kilovolts, a modulation coefficient of 0.82, and a fringe spacing of 5 microns. By comparing the data in Figure 12 with the data in Figure 13, which is for an applied voltage of 3 kilovolts, a modulation coefficient of 0.82, and a fringe spacing of 5 microns, it can be seen that the diffraction efficiency in the 20 to 40 millisecond write time regime for a fringe angle of 90 degrees is within error limits of being the same for both voltages. This result is what the theory predicts as shown in the previous section. When comparing the data in Figure 12 with the data in Figure 14, which is for an applied voltage of 5 kilovolts, a modulation coefficient of 0.45, and a fringe spacing of 5 microns, it can be seen that the

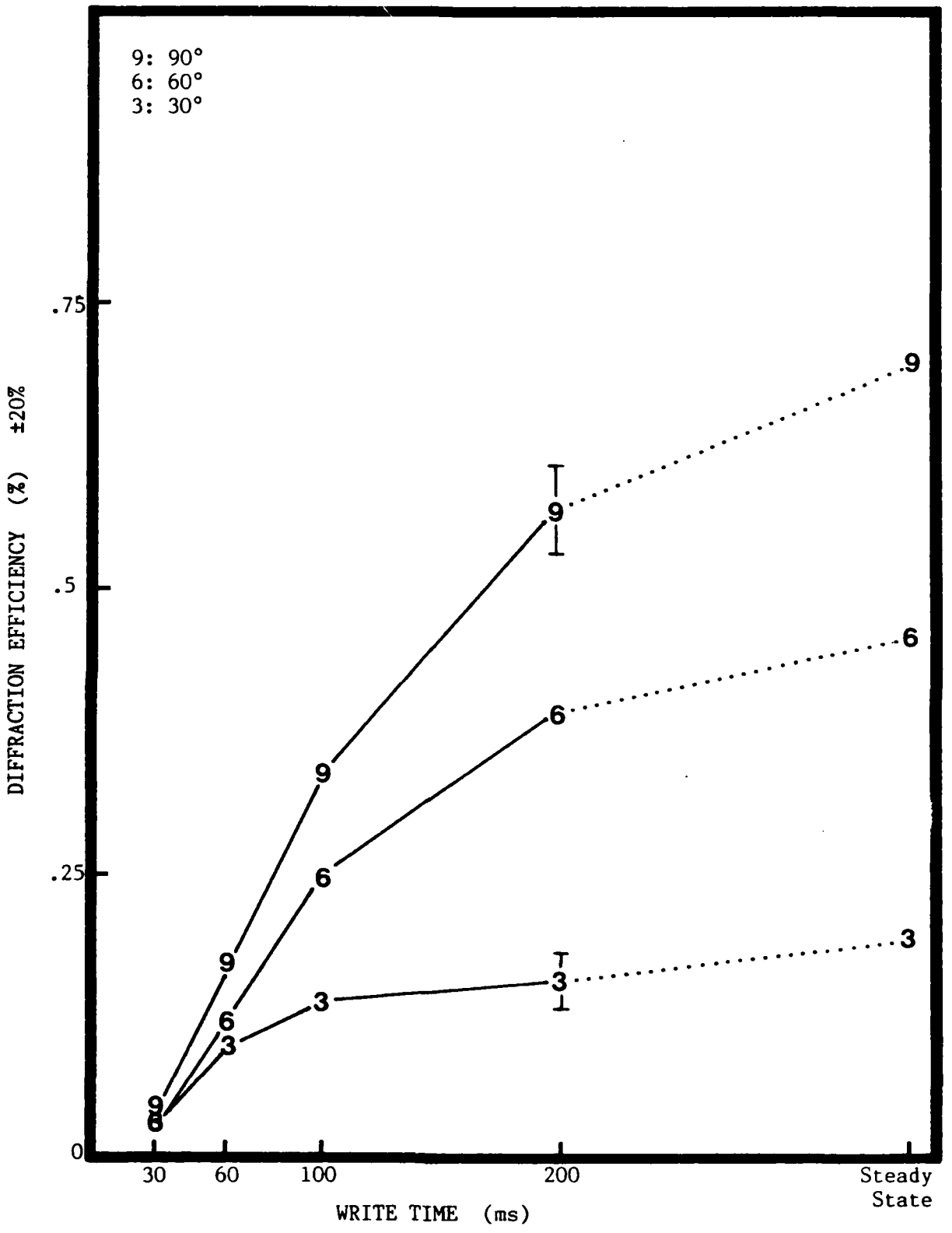

Figure 11. Diffraction efficiency versus write time: M=0.82, V=3kV, Λ=5μ, unpolarized read beam, several fringe angles

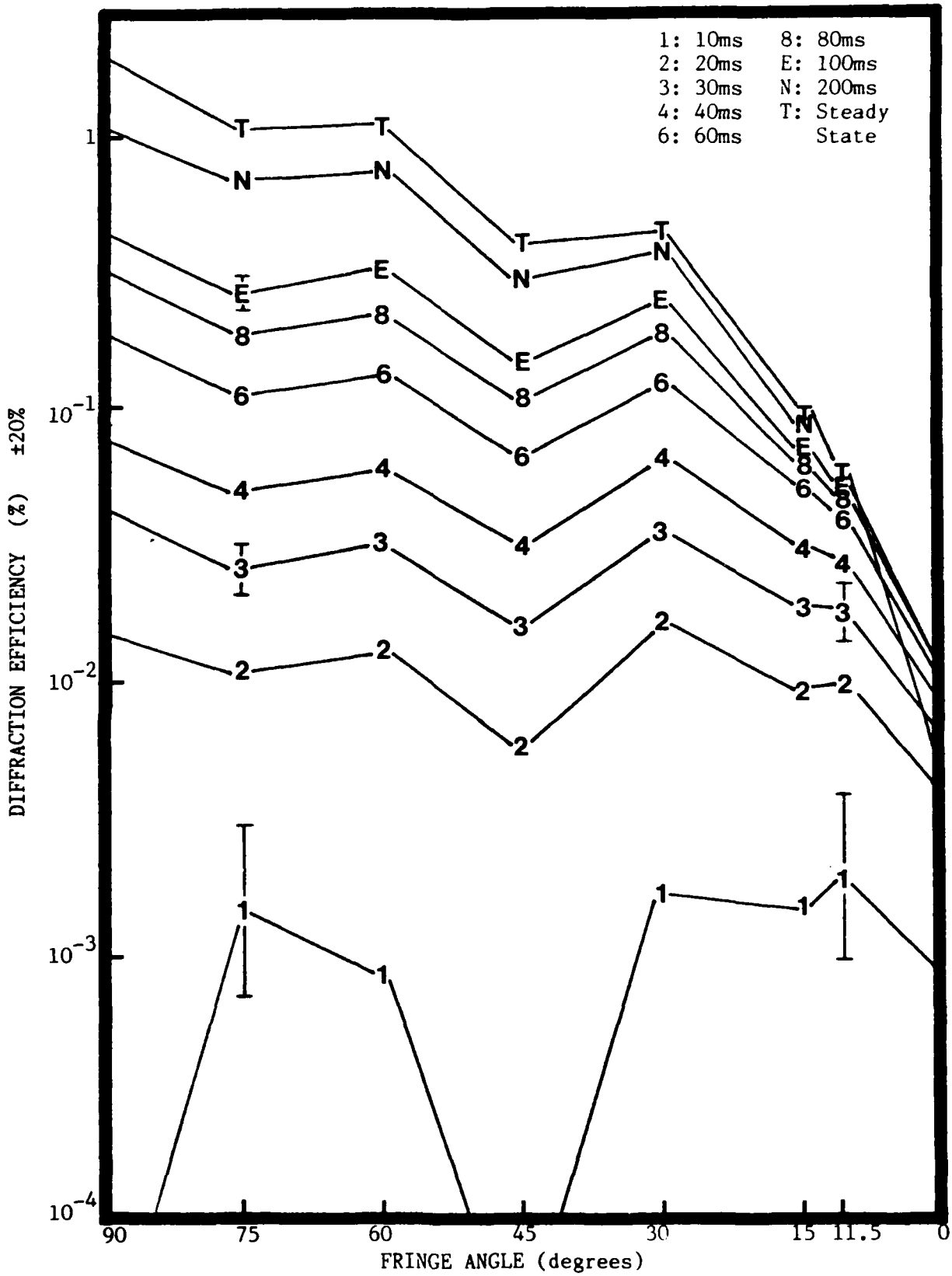

Figure 12. Diffraction efficiency versus fringe angle: M=0.82, V=5kV, Λ=5μ, unpolarized read beam, many write times

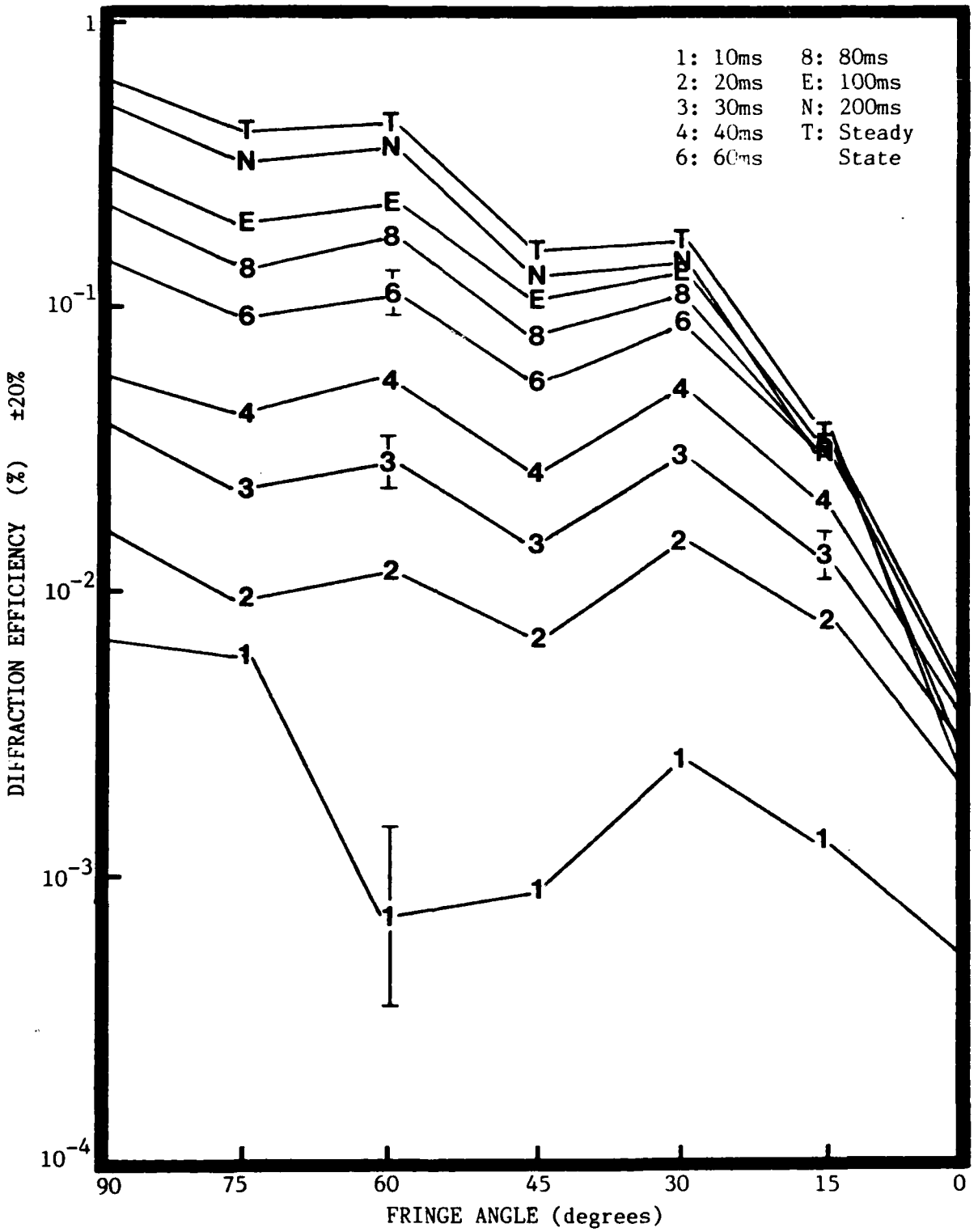

Figure 13. Diffraction efficiency versus fringe angle: M=0.82, V=3kV, Λ=5μ, unpolarized read beam, many write times

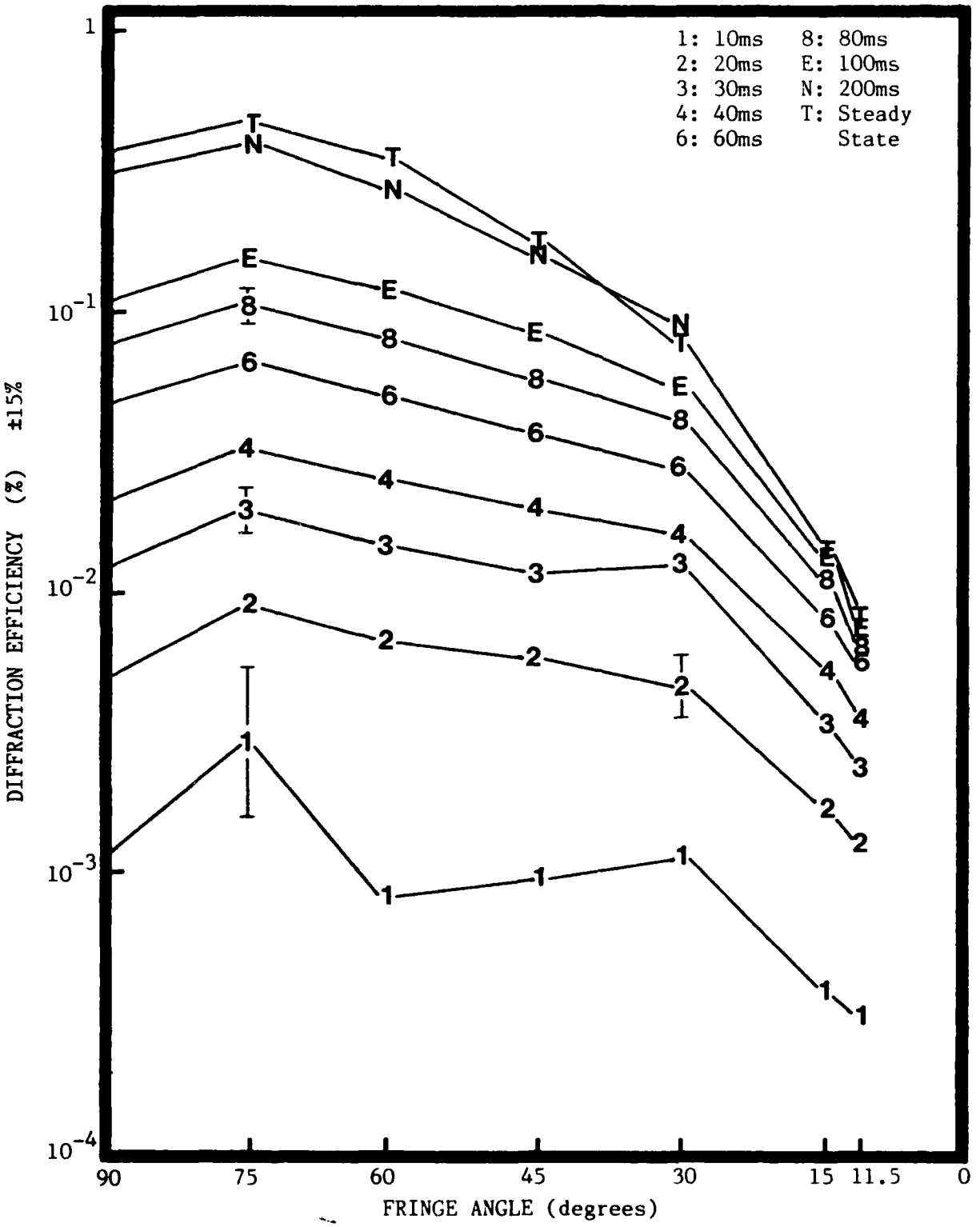

Figure 14. Diffraction efficiency versus fringe angle: M=0.45, V=5kV, Λ=5μ, unpolarized read beam, many write times

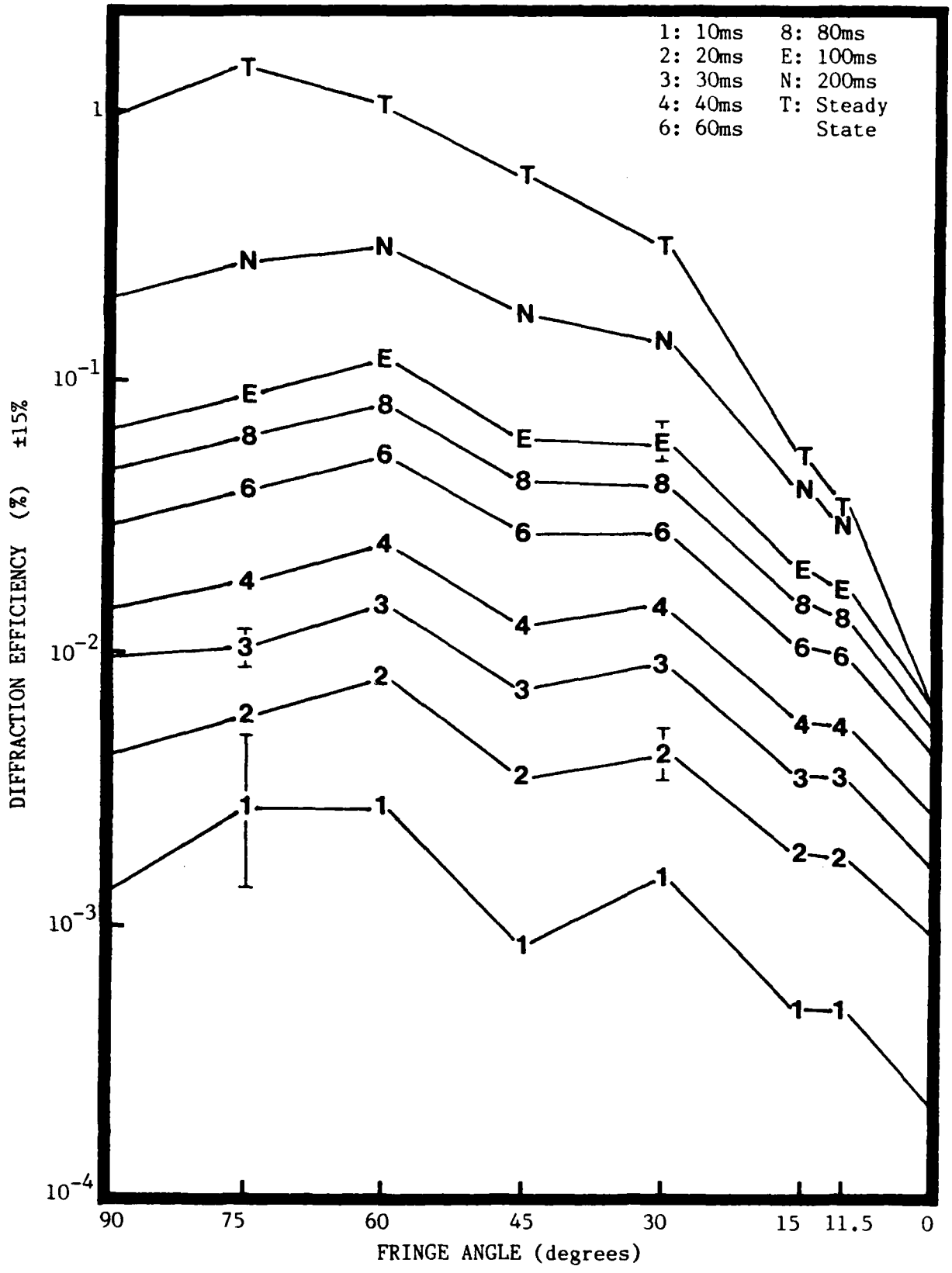

Figure 15. Diffraction efficiency versus fringe angle: M=0.82, V=5kV, Λ=3μ, unpolarized read beam, many write times

diffraction efficiency decreases on the average a factor of 0.29 as the modulation coefficient goes from 0.82 to 0.45 for a fringe angle of 90 degrees and write times of 20 to 40 milliseconds. The decrease is within error limits of the predicted decrease of 0.21.

Finally, when comparing the data in Figure 12 with the data in Figure 15, which is for an applied voltage of 5 kilovolts, a modulation coefficient of 0.82, and a fringe spacing of 3 microns, it can be seen that the diffraction efficiency decreases a factor of 0.24 as the fringe spacing goes from 5 to 3 microns. Again, the comparison is for a fringe angle of 90 degrees and write times of 20 to 40 milliseconds. The decrease is within error limits of the predicted decrease of 0.36.

Referring again to Figures 12, 13, 14, and 15, it can be seen that the diffraction efficiency is about an order of magnitude lower for fringe angles near 0 degrees than for a fringe angle of 90 degrees. This falloff of the diffraction efficiency as the fringes go from being perpendicular to parallel to the applied field occurs for all the values of modulation coefficient, applied voltage, fringe spacing, and exposure times used during the experiment. Therefore, the phenomenon causing the falloff of diffraction efficiency as a function of the fringe angle appears to be independent of these parameters. However, the angular dependence of diffraction efficiency is strongly dependent upon the polarization of the read beam, as shown below.

POLARIZED READ BEAM. A typical plot of data showing the angular dependence of diffraction efficiency for a vertically polarized read beam is shown in Figure 16, and a similar plot is shown in Figure 17 for a horizontally polarized read beam. Both figures are semi-log

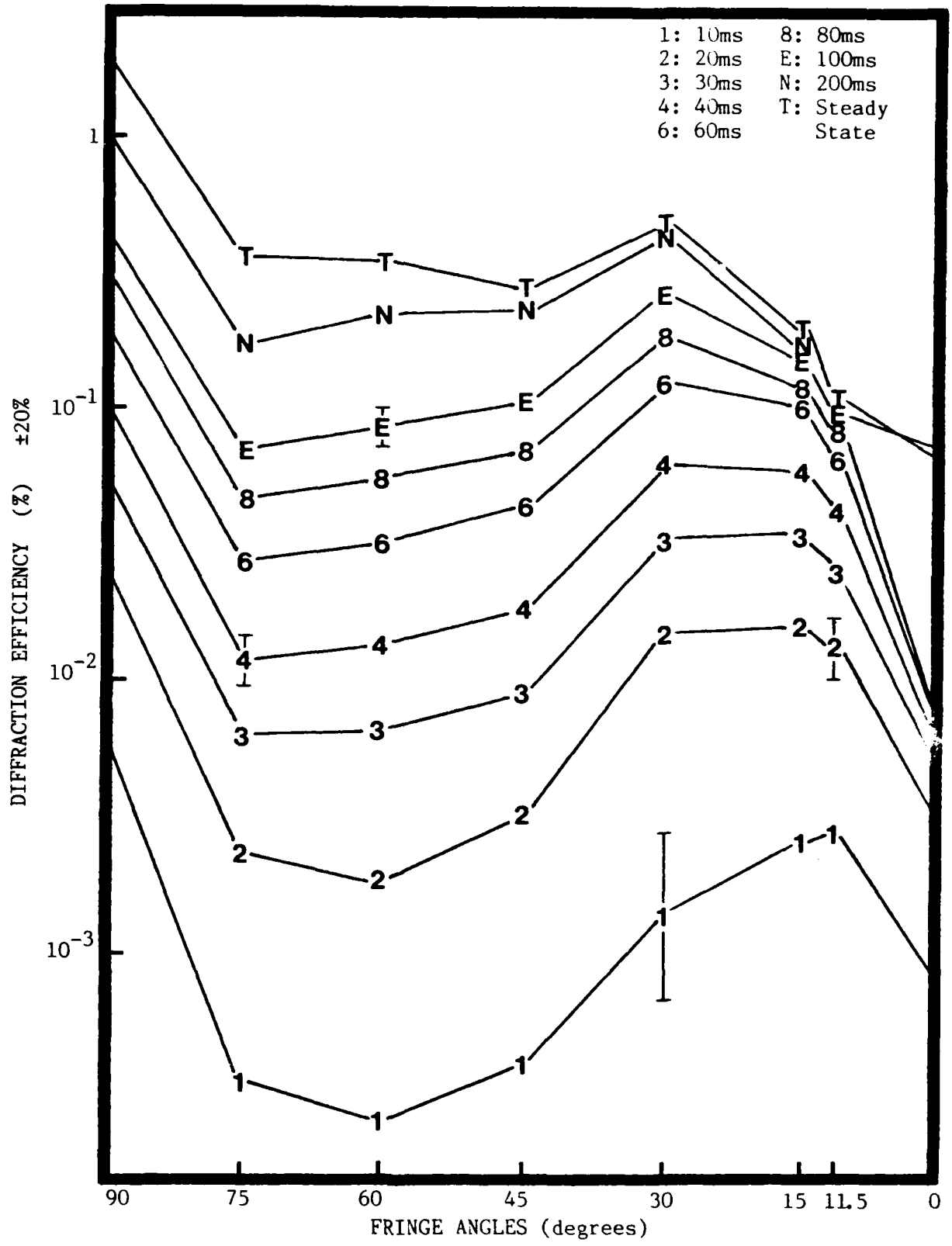

Figure 16. Diffraction efficiency versus fringe angle: M=0.82, V=5kV, Λ=5μ, vertically polarized read beam, many write times

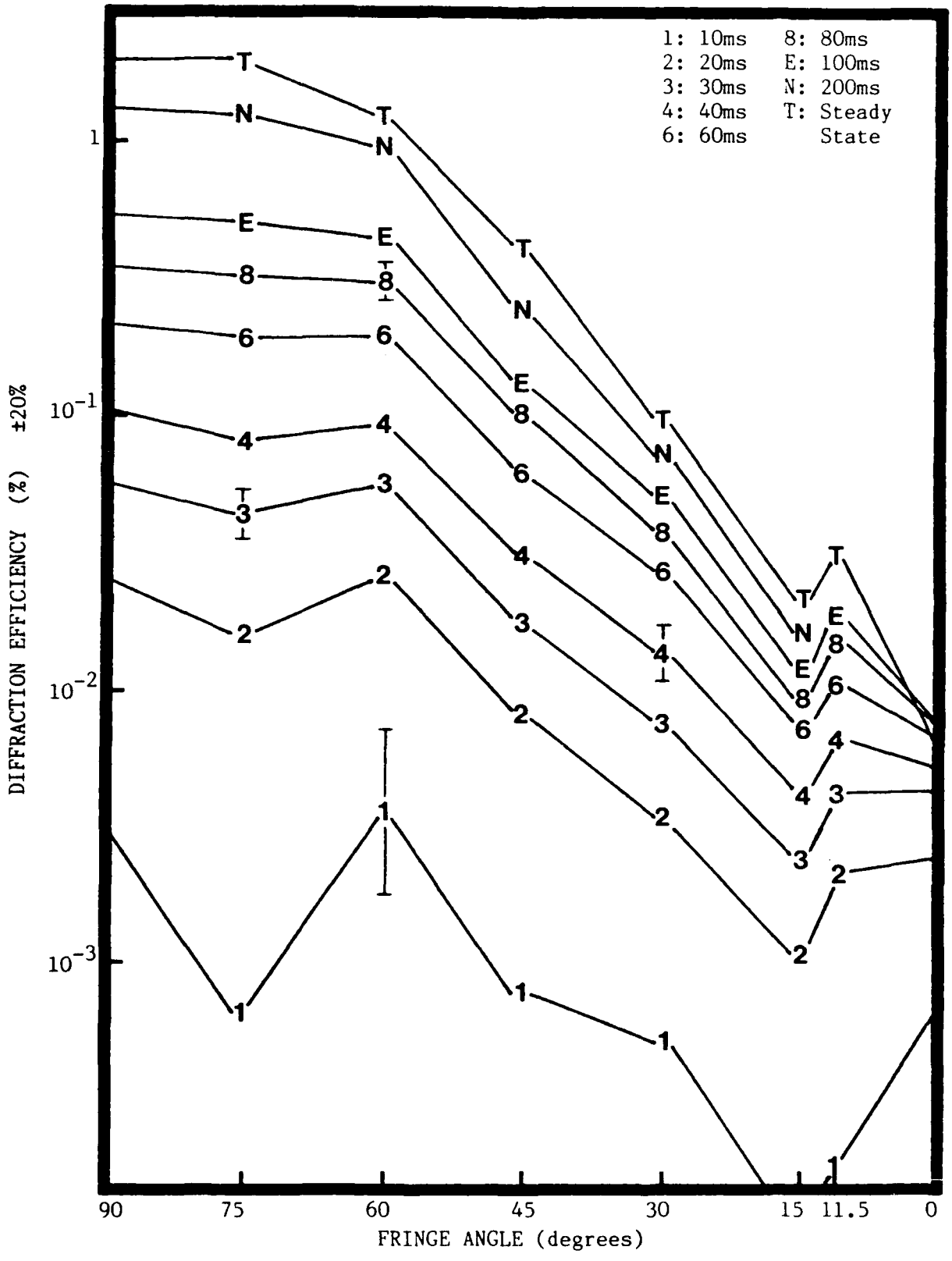

Figure 17. Diffraction efficiency versus fringe angle: M=0.82, V=5kV, Λ=5μ, horizontally polarized read beam, many write times

plots for a wide range of write times with an applied voltage of 5 kilovolts, a fringe spacing of 5 microns, and a modulation coefficient of 0.82. The rest of the tabulated data for both vertically and horizontally polarized read beams can be found in the Appendix. All the short exposure time data for perpendicular fringes fits theoretical predictions within error limits. Both Figure 16 and 17 show that the diffraction efficiency as a function of fringe angle is heavily dependent upon the polarization of the read beam. Figure 18 displays the polarization dependence of diffraction efficiency even more clearly. The diffraction efficiency curves from Figures 16 and 17 for write times of both 40 milliseconds and steady state are plotted on a semi-log plot. The curves corresponding to a horizontal read beam have quite a different shape than the curves corresponding to a vertical read beam.

VOLTAGE SCALING. In the theory chapter, it was mentioned that the component of the applied voltage perpendicular to the fringe pattern was the force that dominated the space charge field formation for short write times. To test this model, diffraction efficiencies were measured for fringe angles between 90 and 0 degrees, and the magnitude of the applied voltage was increased (scaled) as the fringe angle was decreased to keep the component of the applied voltage perpendicular to the fringes constant. Table II contains a list of the scaled voltages for the fringe angles.

Typical diffraction efficiency as a function of fringe angle when using scaled voltages can be found in Figures 19, 20, and 21, and the rest of the data is contained in the Appendix. All the diffraction efficiencies for perpendicular fringes fit theoretical

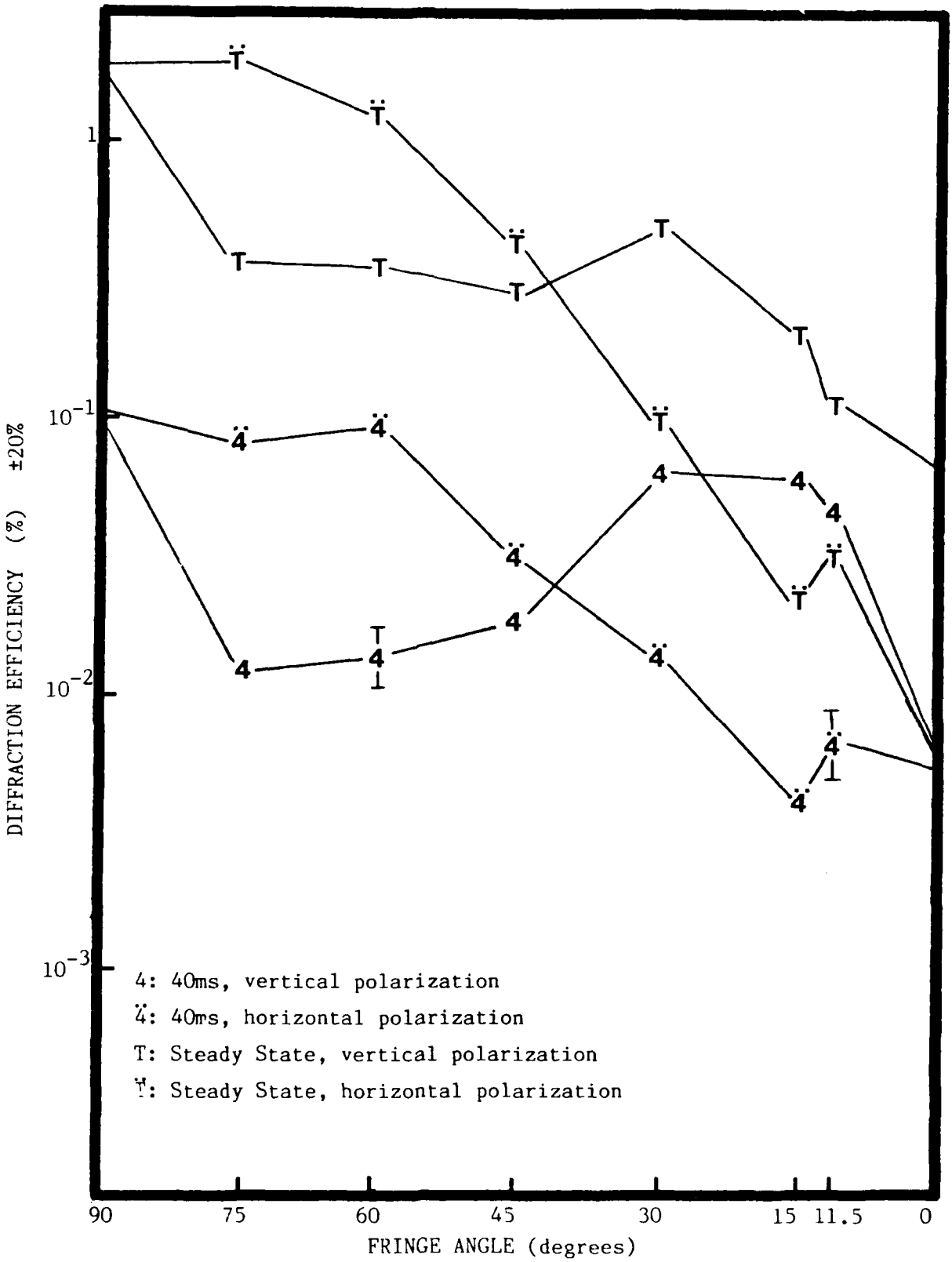

Figure 18. Diffraction efficiency versus fringe angle: M=0.82, V=5kV, Λ=5μ, vertically and horizontally polarized read beam, many write times

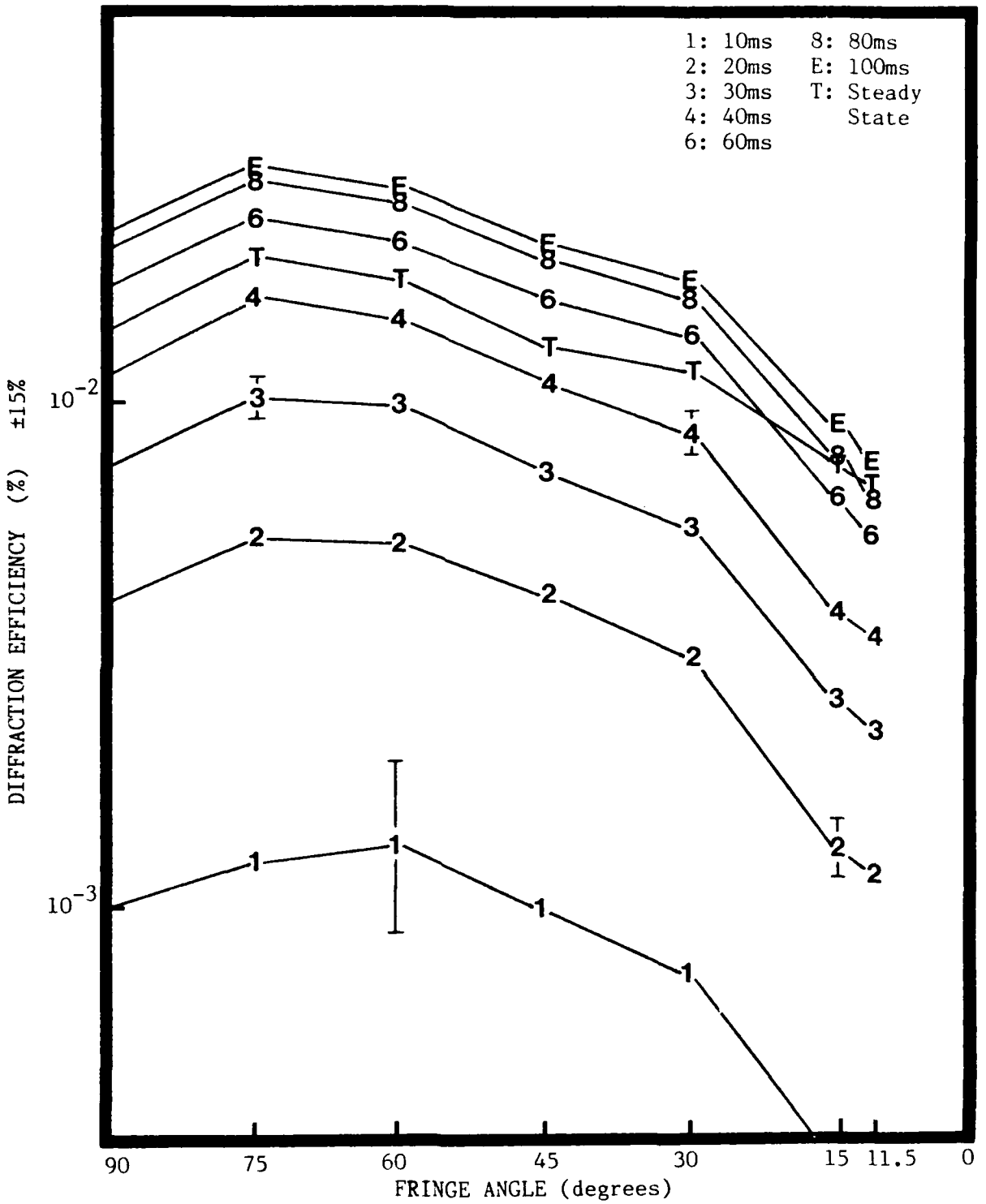

Figure 19. Diffraction efficiency versus fringe angle: M=0.45, scaled V, Λ=5μ, unpolarized read beam, many write times

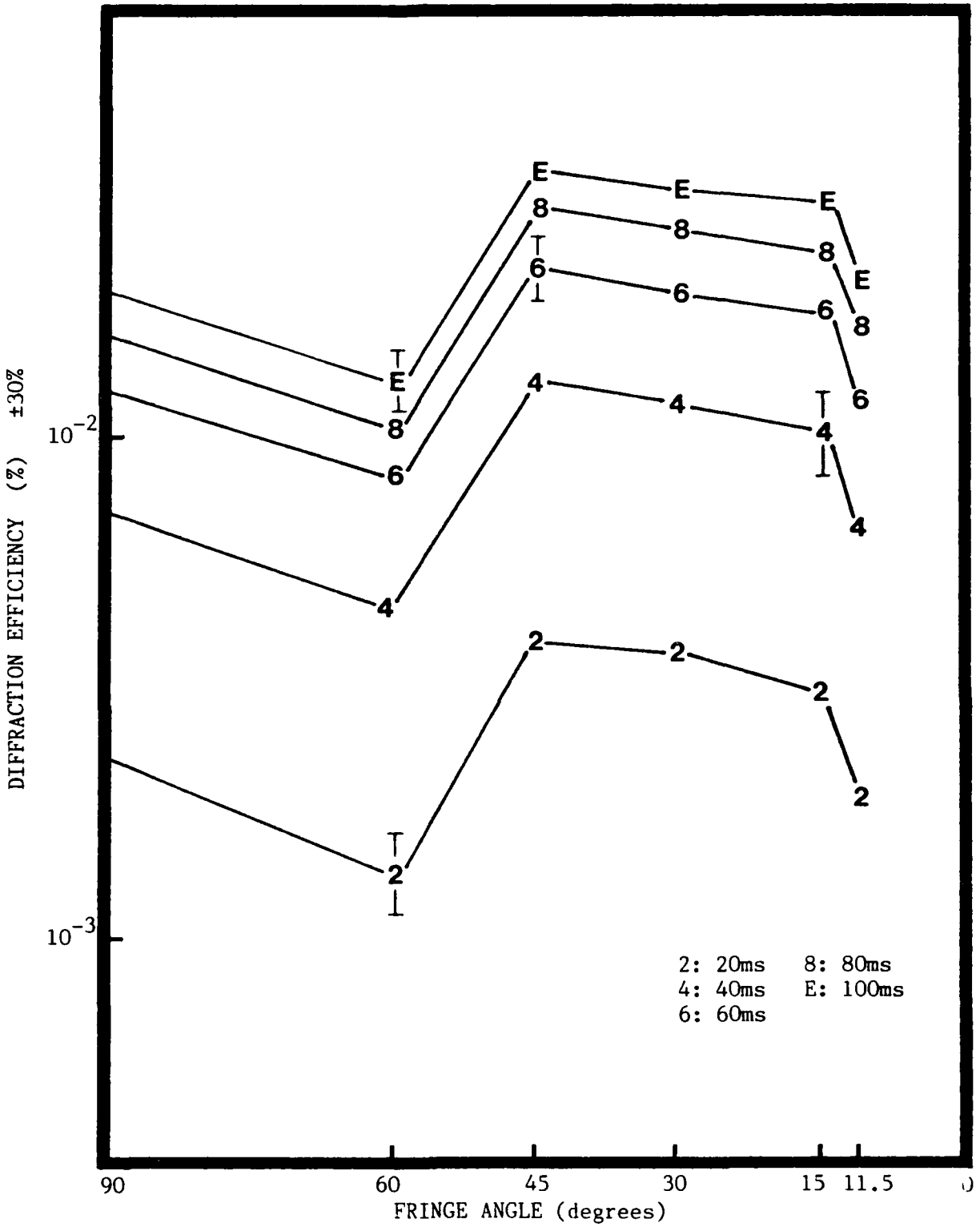

Figure 20. Diffraction efficiency versus fringe angle: M=0.82, scaled V, Λ=3μ, vertically polarized read beam, many write times

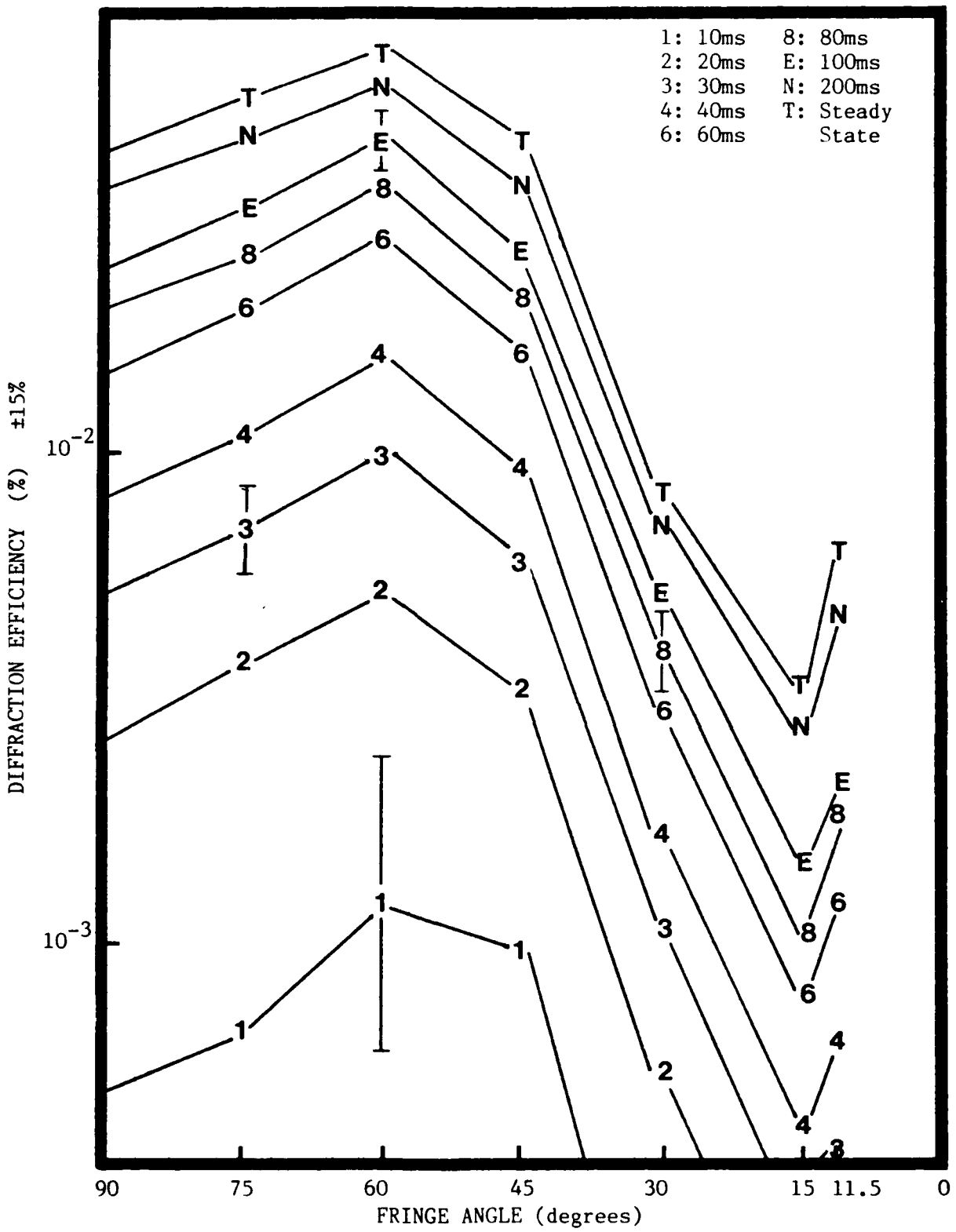

Figure 21. Diffraction efficiency versus fringe angle: M=0.82, scaled V, Λ=3μ, horizontally polarized read beam, many write times

TABLE II

Scaled Voltages

Fringe angle (degrees)	Voltage (kV)
90.0	1.00
75.0	1.04
60.0	1.15
45.0	1.41
30.0	2.00
15.0	3.86
11.5	5.00

predictions. Figure 19 is for a fringe spacing of 5 microns, a modulation coefficient of 0.45, and for an unpolarized read beam. Figure 20 is for a fringe spacing of 3 microns, a modulation coefficient of 0.82, and vertical read beam polarization. Figure 21 has the same values for the parameters as Figure 20 except that the read beam is horizontally polarized.

If the theory mentioned above was the only factor influencing the angular dependence of the diffraction efficiency, the diffraction efficiency should become independent of the angle when the applied voltage is scaled to the angle. By looking at Figures 19-21, it can be seen that the diffraction efficiency still varies as the fringe angle varies. However, that should be expected, since the diffraction efficiency has already been shown to depend strongly upon the polarization of the read beam; however, the effect of read beam polarization only affects the magnitude of the response, not the response time

of the BSO crystal. Figure 22 illustrates this quite well. Diffraction efficiencies from Figure 21 are plotted as a function of time for a variety of fringe angles on a log-log graph for a horizontally polarized read beam, and the slopes of the lines are independent of the fringe angle, showing that the response times are independent of the fringe angle when the voltage is scaled. The lines are shifted on the graph by an additive amount, indicating that although the scaled voltage theory accounts for the angular dependence of the response time when the applied voltage is a constant, there is a multiplicative factor which scales the magnitude of the response for which the scaled voltage theory does not account. Figure 23 is a plot of the same data as in Figure 22, with the curves for all the fringe angles shifted vertically to overlay the curve corresponding to a fringe angle of 90 degrees. The multiplicative factor shifting each curve is listed in Table III. This makes it even clearer that the response times of the crystal for scaled voltages stays the same for all angles, and for well into the write cycle.

Figure 24 is a plot of diffraction efficiency versus time for a variety of angles, with the data taken from Figure 20. The curves are shifted vertically, as for Figure 23, and the response times are again evidently the same for all fringe angles. The multiplicative factor shifting each curve is listed in Table IV. Figure 24 demonstrates that the voltage scaling effect upon the response time of the crystal is reproducible, since the data for Figure 24 was taken weeks before the data for Figure 23. In between the two data runs, equipment on the table had been shifted about quite a bit, and yet the results of voltage scaling remained the same.

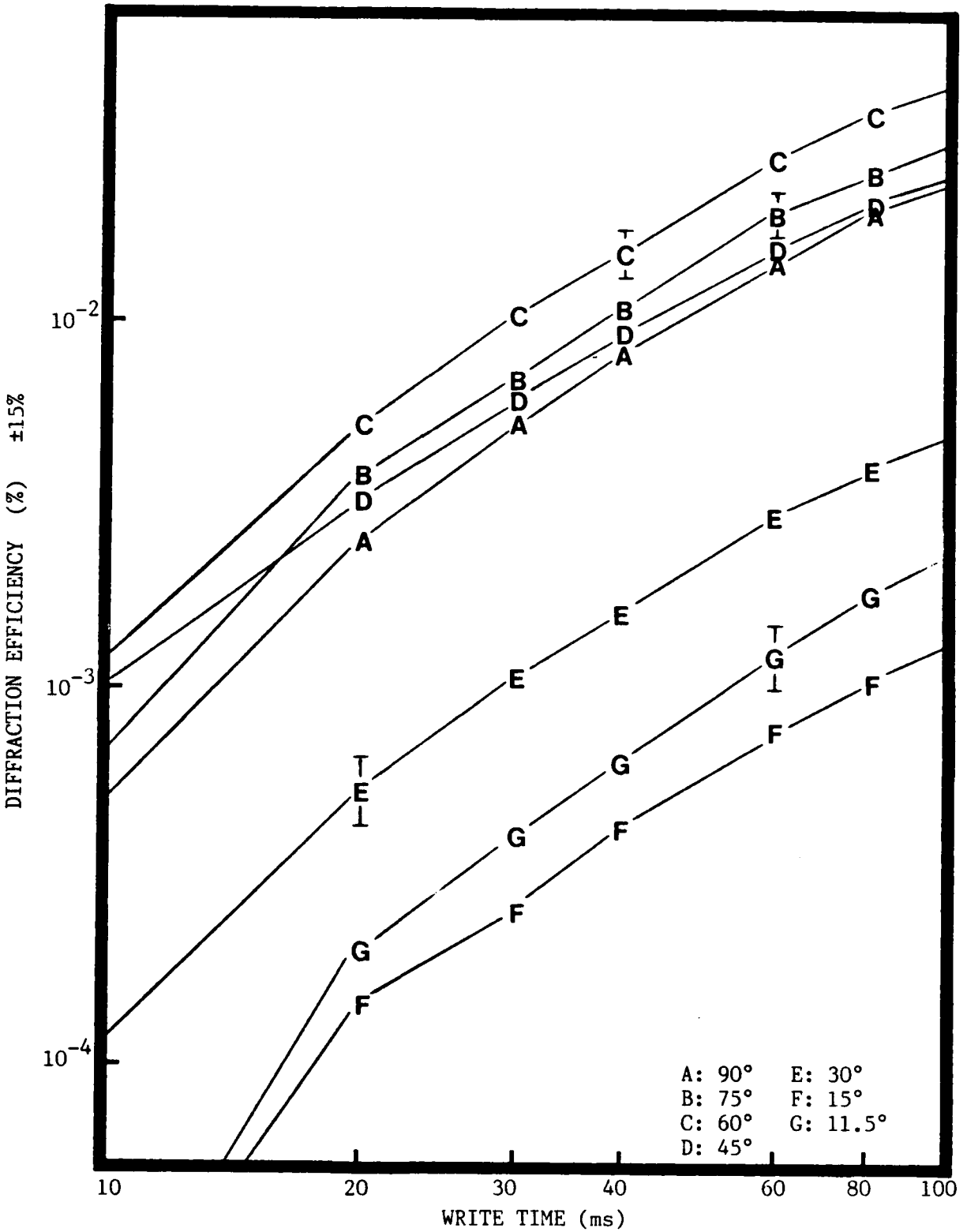

Figure 22. Diffraction efficiency versus write time: M=0.82, scaled V, Λ=3μ, horizontally polarized read beam, many fringe angles

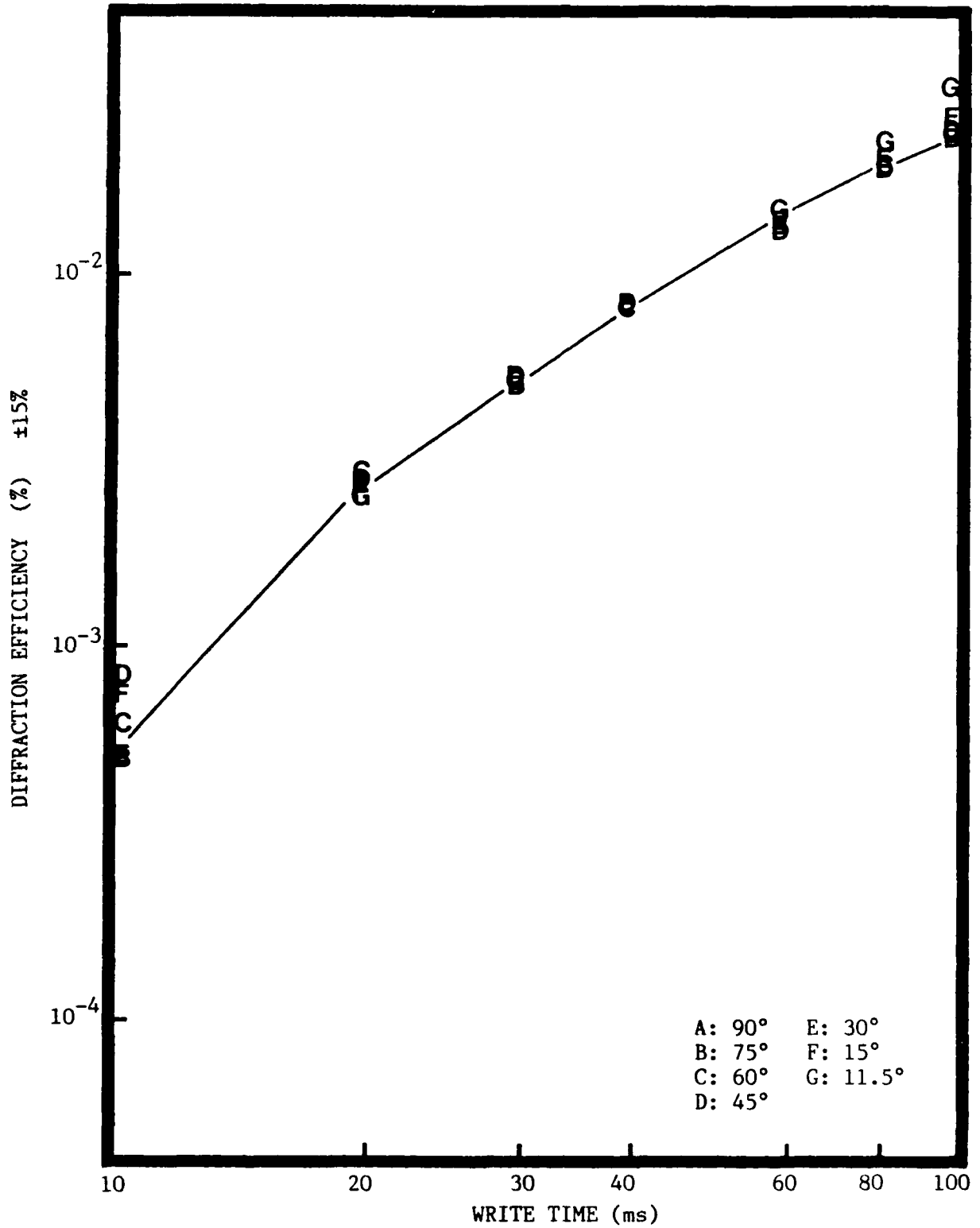

Figure 23. Diffraction efficiency versus write time: M=0.82, scaled V, Λ=3μ, horizontally polarized read beam, many fringe angles, shifted curves

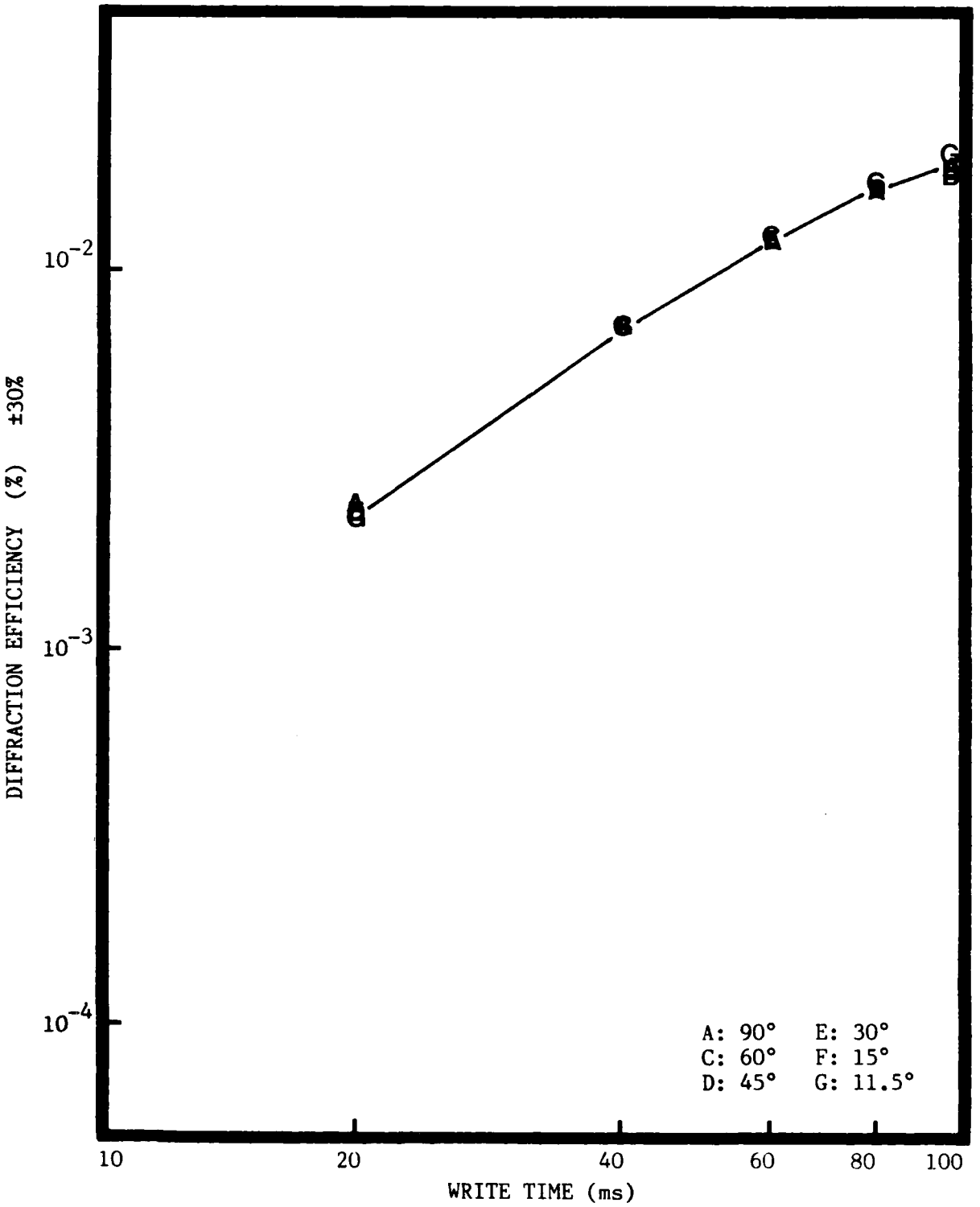

Figure 24. Diffraction efficiency versus write time: M=0.82, scaled V, Λ=3μ, vertically polarized read beam, many fringe angles, shifted curves

TABLE III

Multiplicative Shift Factors for Figure 23

Fringe Angle (degrees)	Vertical Shift
90.0	1.00
75.0	1.36
60.0	1.91
45.0	1.16
30.0	0.21
15.0	0.052
11.5	0.080

Polarization effects appear to have great promise in explaining the multiplicative factor affecting the magnitude of the response time of the crystal, but strict analytical explanations would require extensive numerical analysis. To accurately determine the polarization

TABLE IV

Multiplicative Shift Factors for Figure 24

Fringe Angle (degrees)	Vertical Shift
90.0	1.00
60.0	0.64
45.0	1.75
30.0	1.60
15.0	1.43
11.5	0.93

effect upon the diffraction efficiency, the direction and magnitude of the total electric field must be known at every point in the crystal. The resultant electric field is the vectorial sum of the applied field generated by the applied voltage and the space charge field, but since the time development of the space charge field in the crystal is highly complex, accurate expressions for the effect of read beam polarizations are beyond the scope of this thesis.

A simplifying approximation for the electric field in the crystal is to assume that the only field existing in the crystal is perpendicular to the fringes and periodic in the direction of the normal to the fringe pattern. Then, using the expressions developed by M. P. Petrov (Ref. 11) and assuming that the electric field in the crystal remains constant when the applied voltage is scaled, the change in the diffraction efficiency of the crystal due to polarization effects can be calculated. There are two reasons why the polarization effects of the read beam need to be accounted for in this experiment. The first is because the BSO crystal is being rotated to achieve varied fringe angles instead of the fringe pattern being rotated. Since the read beam polarization is kept constant, the angle between the polarization of the read beam and the crystallographic axes of the crystal changes for every fringe angle. Also, as the angle of the fringe pattern on the crystal changes with respect to the crystallographic axes, the directions of the propagation modes and the change in magnitude of the index of refraction for each of those propagation modes also changes.

Figure 25 is a plot of both the vertical displacements listed in Table III and the calculated displacement values as a function

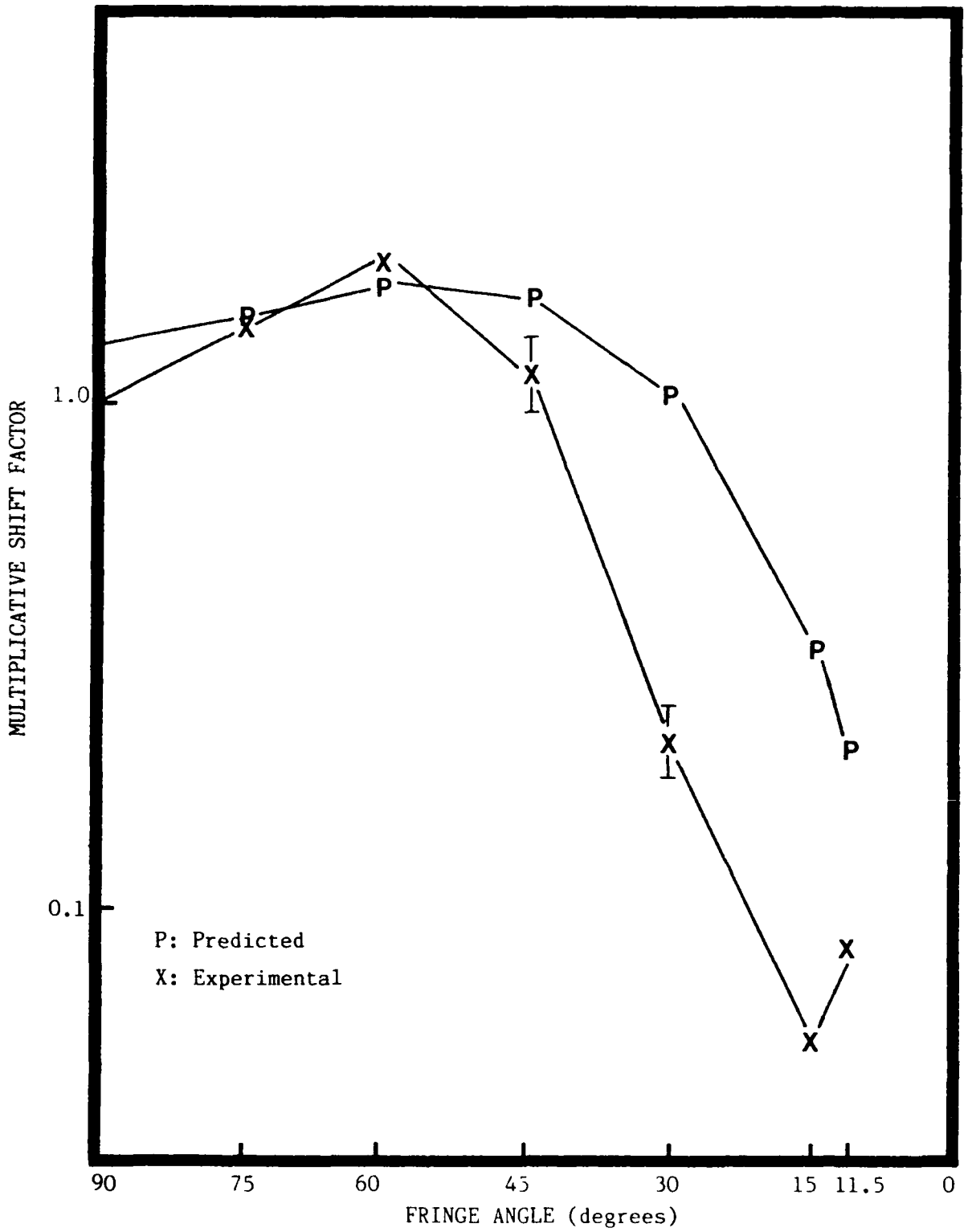

Figure 25. Plot of predicted and experimental multiplicative shift factors versus fringe angle: M=0.82, scaled V, horizontally polarized read beam, Λ=3μ

of fringe angle. There is good semiquantitative agreement for fringe angles greater than 60 degrees, and qualitative agreement for smaller angles.

Figure 26 is a plot of both the vertical displacements listed in Table IV and the calculated displacement values as a function of fringe angle. There is good semiquantitative agreement for fringe angles larger than 60 degrees, but the curves lack even a qualitative agreement for smaller fringe angles.

In conclusion, the diffraction efficiency of a thick hologram in a BSO crystal is a function of the applied voltage, the modulation coefficient, the fringe spacing, the polarization of the read beam, and the fringe angle. There did not appear to be a significant angular dependence that the modulation coefficient, applied voltage, or the fringe spacing had upon the diffraction efficiency. The dominate effects causing the angular dependence of diffraction efficiency are the falloff of the effect that the applied voltage has upon the space charge field formation and the orientation of the read beam polarization. The theory describing the falloff of the effect of the applied voltage upon the space charge field formation accounts for the angular dependence of the response time of the crystal, and polarization effects appear to give a rough approximation for the magnitude of the response.

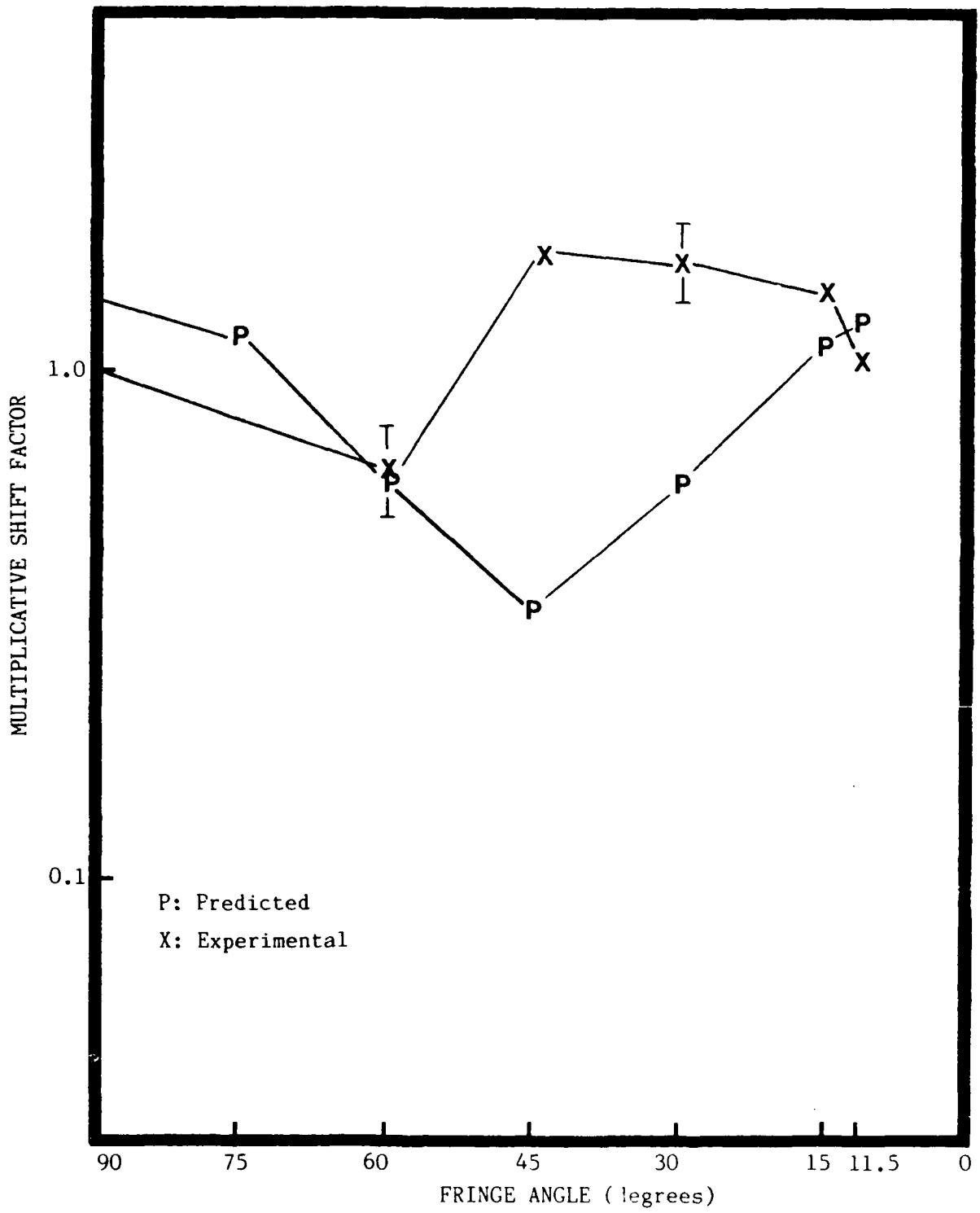

Figure 26. Plot of predicted and experimental multiplicative shift factors versus fringe angle: M=0.82, scaled V, vertically polarized read beam, Λ=3μ

VI. APPLICATIONS

A. IMPLICATIONS OF ANGULAR DEPENDENCE OF DIFFRACTION EFFICIENCY

As mentioned in the introduction, holographic fringes tend to be oriented in one direction when the angle between the reference and object beams is more than a few degrees. As the angle between the two beams decreases, the fringes become less preferentially oriented in one direction. Many important applications using BSO as a holographic storage medium, such as phase conjugation and optical image processing, have reference-object beam angular separations of only a few degrees. In the limit as the reference and object beams become on-axis with no angular separation, fringes can have any orientation.

To analyze further the effect of angular dependence of diffraction efficiency, consider the case of a hologram formed in BSO from an on-axis point source interfering with an on-axis plane wave reference beam. The resulting fringe pattern is a series of concentric circles, forming a zone plate. The fringe spacing of a zone plate decreases as one moves from the center of the plate outward. For the case of a thick sinusoidal index of refraction change which occurs for short write times, the zone plate acts like a lens, diffracting part of a collimated light beam into a diverging wave which appears to come from a virtual point source on the other side of the

plate. Most of the light does not get diffracted, since BSO typically has a diffraction efficiency on the order of 1%.

Since fringes at 0 degrees have diffraction efficiencies which are an order of magnitude less than for fringes at 90 degrees, distortion will occur in the reconstructed point source when the hologram is illuminated with a plane wave reference beam. If the zone plate fringes were uniformly recorded in the crystal, the point source would be an Airy disk diffraction pattern. However, since the fringes are not uniformly recorded, distortions will occur in the diffraction pattern. Consider dividing the zone plate into four regions - two where the fringes strongly diffract, and two where the fringes weakly diffract. These regions will be wedge-shaped, with the two strongly diffraction regions oriented parallel to the applied field, and the two weakly diffracting regions oriented perpendicular to the applied field (see Figure 27). The lines dividing these regions intersect the zone plate fringe pattern through the fringes that have a diffraction efficiency which is 10 decibels down from the diffraction efficiency of fringes perpendicular to the applied field. The 10 decibel line was chosen as a figure of merit; other figures of merit can also be selected. As an example, the angle θ has a value of around 140 degrees for the data in Figure 14. The strongly diffracting regions dominate the formation of the diffraction pattern, and cause the pattern to be a two beam interference pattern of some sort, since light diffracted from the two weakly diffracting regions is negligible.

Another factor to consider for practical applications of BSO is spatial frequency response. J. P. Huignard (Ref. 13) has shown experimentally that the spatial frequency response of BSO in the

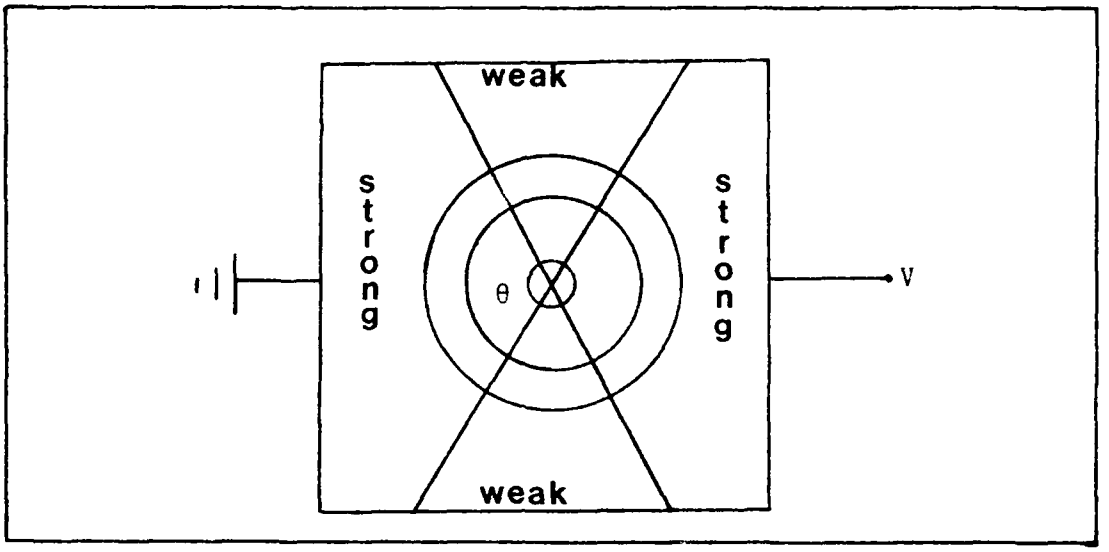

Figure 27. Strongly and weakly diffracting regions of a zone plate recorded in BSO

steady state regime depends upon the magnitude of the applied field as predicted by theory developed by Kukhtarev et al., (Ref. 14, 15). In Figure 28, wavefront reflectivity is plotted versus fringe spacing for several values of the applied field when fringes are perpendicular to the applied field. Wavefront reflectivity is a quantity similar to diffraction efficiency. Again using the zone plate example, it can be seen that for an applied field of greater than 2 kilovolts/cm, the center of the zone plate will diffract more strongly than the edges. For an applied field of 2 kilovolts/cm, all of the zone plate will diffract equally well. Finally, for an applied field of less than 2 kilovolts/cm, the edges of the zone plate will diffract more strongly than the center. The spatial frequency characteristics of BSO will also distort the reconstructed point source formed by the zone plate.

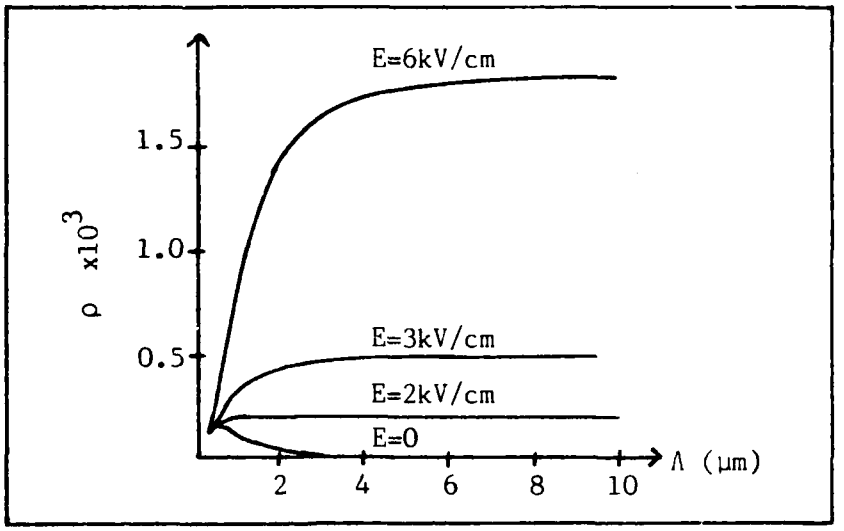

Figure 28. Wavefront reflectivity ρ versus fringe spacing Λ for several values of applied field E

B. SPECIFIC APPLICATIONS

The effects of angular and spatial frequency dependence of diffraction efficiencies in BSO should be taken into account for specific applications of BSO. Such considerations are beyond the scope of this thesis. However, several specific applications will be presented in this section to emphasize the potential usefulness of BSO as a quick-response holographic storage medium.

One area in which BSO is finding application is in phase conjugate wavefront generation (Ref. 16). Phase conjugation techniques can be used to restore a distorted wavefront to its original, undistorted condition. Consider the setup in Figure 29 (Ref. 17). An image, formed by illuminating the object slide with a plane wave, is passed through an aberrating medium, severely distorting the original wavefront. This distorted wavefront, forming an object beam,

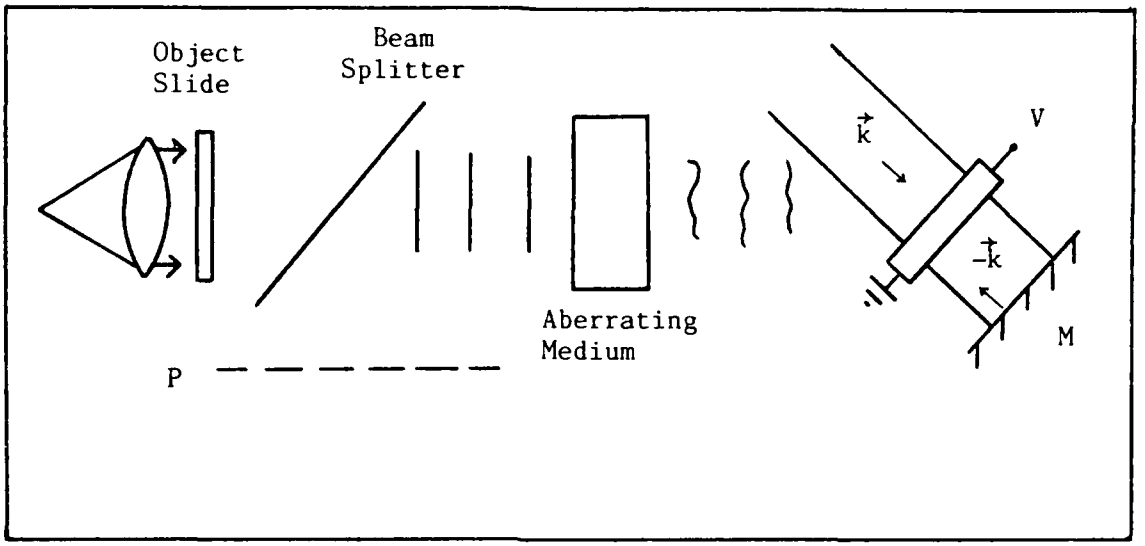

Figure 29. Setup for phase conjugate wavefront generation

and a plane wave reference beam interfere upon the BSO crystal, producing a hologram. To play back the hologram, mirror M is placed behind the crystal, retroreflecting the reference beam. One of the waves formed by illuminating the hologram in this manner is the phase conjugate of the object beam, and this conjugate wave propagates back along the object beam path through the aberrating medium. The aberrating medium introduces distortions into the phase conjugate wave, which serve to remove the distortions previously caused by the medium. When the phase conjugate wave emerges from the aberrating medium, all distortions have been removed from the wave if no energy is scattered out of the system. The resulting intensity pattern seen in plane P from the undistorted phase conjugate of the original image transmitted is the same as the intensity pattern of the original image. Because BSO is a reusable, quick-response holographic storage medium,

the image and the aberrating medium can be time varying. Uses of phase conjugation techniques for applications ranging from laser fusion to optical resonators (Ref. 18) have been suggested.

The phase conjugation setup described above requires that the phase conjugate of the distorted image be propagated back through the aberrating medium. For one-way transmission of energy, this technique could not be used. A means of reducing image distortion for one-way image transmission through an aberrating medium has been proposed (Ref. 19), which only requires a small portion of the distorted wavefront to be reflected from the target back to the transmitter. A BSO crystal is used in a manner similar to the phase conjugation technique described earlier, and the transmitted image beam is intentionally distorted in such a way that the aberrating medium between the transmitter and the target will remove most of the distortions, producing a clearer image at the target than without this corrective technique. One possible application of this technique is in the area of atmospheric transmission of high energy laser beams. For example, consider the case of a laser beam weapon used to shoot down an enemy aircraft. Distortions induced by the atmosphere reduce the power density of the laser beam upon the target. However, if part of the aircraft reflects back some of the laser beam to the transmitter, the above technique might be used to reduce atmospheric distortions and increase the power density of laser light upon the aircraft.

Another application of BSO is in the area of interferometry using holographic techniques. Because BSO does not have to be developed to acquire the hologram the way photographic film does, and

because of BSO's millisecond response time, interferometry can be done very quickly and easily. Also, BSO can be used even in the saturation regime, whereas film must be properly exposed to be useful.

Finally, it has been shown that BSO can be used in real time image processing. J. O. White and A. Yariv (Ref. 2) constructed a non-linear optical processor and demonstrated that the processor could be used for spatially convolving and correlating images. In the referenced paper, the authors mentioned that the processor might be successfully used for analyzing tissue samples for cancer cells.

VII. CONCLUSIONS AND RECOMMENDATIONS

The change in diffraction efficiency as a function of the angle of the fringe pattern was studied in the experiment for this thesis for a variety of parameters. This section will present the conclusions reached for the data obtained, and recommendations for further study. Since the manufacture of controlled impurity BSO crystals is still unperfected, crystal response will vary between crystals. The results obtained in this study were for only one crystal sample, so no attempt has been made to generalize these results.

The conclusions are:

(1) The efficiency of thick birefringent phase diffraction gratings in BSO crystals falls off by an order of magnitude for fringes parallel to the applied field compared to fringes perpendicular to the applied field.

(2) The two dominant factors influencing this dropoff in diffraction efficiency are the effect that the space charge field has upon inducing index of refraction changes in the crystal and the falloff in the effect that the applied field has upon the space charge field formation.

(3) For short write times, the effect of the applied field upon the space charge pattern formation falls off as the cosine of the angle between the fringe pattern and the applied field. This

accounted for the angular dependence of the response times of the crystal, but not the magnitude of the response.

(4) Polarization effects from the read beam give an order of magnitude explanation for the angular dependence of the magnitude of the crystal response.

It is recommended that a computer study be done to detail the time development of the space charge field inside BSO crystals for an arbitrary angle of the fringe pattern. This would allow accurate calculations to be done to analyze the effects of space charge field orientation upon the efficiency of thick phase diffraction gratings in BSO. Also, work should be done to generalize Kogelnik's theory on thick diffraction gratings to birefringent gratings.

Bibliography

1. Huignard, J. P. and F. Micheron. "High-Sensitivity Read-Write Volume Holographic Storage in $Bi_{12}SiO_{20}$ and $Bi_{12}GeO_{20}$ Crystals," Applied Physics Letters, 29 (9): 591-593 (November 1, 1976).

2. White, Jeffrey O. and Amnon Yariv. "Real-Time Image Processing via Four-Wave Mixing in a Photorefractive Medium," Applied Physics Letters, 37 (1): 5-7 (July 1, 1980).

3. Huignard, J. P., J. P. Herriau and G. Rivet. "Phase-Conjugation and Spatial-Frequency Dependence of Wavefront Reflectivity in $Bi_{12}SiO_{2}$ Crystals," Optics Letters, 5 (3): 102-104 (March 1980).

4. Peltier, M. and F. Micheron. "Volume Hologram Recording and Charge Transfer Process in $Bi_{12}SiO_{20}$ and $Bi_{12}GeO_{20}$," Journal of Applied Physics, 48 (9): 3683-3690 (September 1977).

5. Tanguay, Armand R., Jr. The Czochralski Growth and Optical Properties of Bismuth Silicon Oxide. PhD dissertation. Boston, MA: Yale University, December 1977.
[The dissertation is available from University Microfilms International.]

6. Moharam, M. G., T. K. Gaylord, R. Magnusson, and L. Young. "Holographic Grating Formation in Photorefractive Crystals with Arbitrary Electron Transport Lengths," Journal of Applied Physics, 50 (9): 5642-5651 (September 1979).

7. Kogelnik, Herwig. "Coupled Wave Theory for Thick Hologram Gratings," Bell System Technical Journal, 48 (9): 2909-2947 (November 1969).

8. Su, S. F. and T. K. Gaylord. "Calculation of Arbitrary-Order Diffraction Efficiencies of Thick Gratings with Arbitrary Grating Shape," Journal of the Optical Society of America, 65 (1): 59-64 (January 1975).

9. Woods, Charles L. Private communication. Rome Air Development Center, Hanscom AFB, MA, July 1983.

10. Yariv, Amnon. Introduction to Optical Electronics. New York: Holt, Rinehart, and Winston, 1976.

11. Petrov, M. P. and A. V. Khomenko. "Anisotrophy of the Photorefractive Effect in $Bi_{12}SiO_{20}$ Crystals," Soviet Physics Solid State, 23 (5): 789-792 (May 1981).

12 Newport Research Corporation. Product catalog for 1980-1981. Fountain Valley, CA.

13. Huignard, J. P., J. P. Herriau, and G. Rivet. "Phase-Conjugation and Spatial-Frequency Dependence of Wavefront Reflectivity in $Bi_{12}SiO_{20}$ Crystals," Optics Letters, 5 (3): 102-104 (March 1980).

14. Kuhktarev, N.V. et al. "Holographic Storage in Electro-Optic Crystals - 1. Steady State," Ferroelectrics, 22 (3-4): 949-960 (1979).

15. Kuhktarev, N. V. et al. "Holographic Storage in Electro-Optic Crystals - 2. Beam Coupling - Light Amplification," Ferroelectrics, 22 (3-4): 961-964 (1979).

16. Yariv, Amnon. "Phase Conjugate Optics and Real-Time Holography," IEEE Journal of Quantum Electronics, QE-14 (9): 650-660 (September 1978).

17. Huignard, J. P. and J. P. Herriau. "Phase Conjugation and Degenerate Four Wave Mixing in Photorefractive $Bi_{12}SiO_{20}$ Crystal," AGARD Conference Proceedings, no. 300: pages (36-1) to (36-6), 1981.

18. Concetto R. Giuliano. "Applications of Optical Phase Conjugation," Physics Today: (April 1981).

19. Ikeda, Osamu, Tohru Suzuki, and Takuso Sato. "Image Transmission Through a Turbulent Medium Using a Point Reflector and Four-Wave Mixing in BSO Crystal," Applied Optics, 22 (14): 2192-2195 (15 July 1983).

APPENDIX

Experimental Data Graphs

This appendix contains graphs of experimental data referred to but not presented in chapter V. Each graph is a plot of diffraction efficiency versus fringe angle for a variety of exposure (write) times, with the other parameters such as fringe spacing and modulation coefficient held constant for each graph. For some of the graphs, the applied voltage is held constant, while for other the applied voltage is scaled with the fringe angle. The magnitude of the applied voltage for each fringe angle for the case of a scaled applied voltage can be found in Table II, page 61. A fringe angle of 90 degrees corresponds to fringes perpendicular to the applied field, and a fringe angle of 0 degrees corresponds to fringes parallel to the applied field.

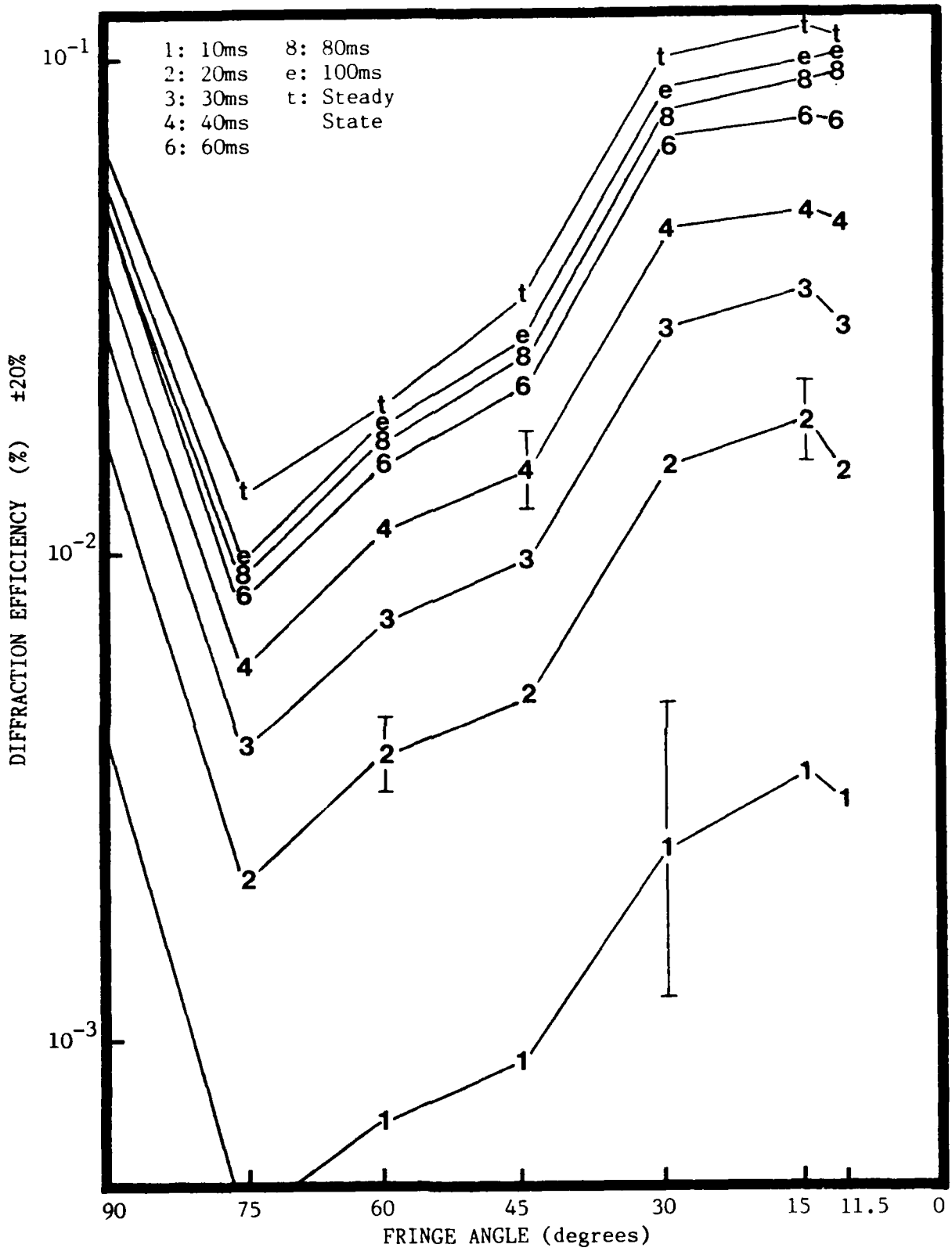

Figure 30. Diffraction efficiency versus fringe angle: M=0.82, scaled V, $\Lambda = 5\mu$, vertically polarized read beam, many write times

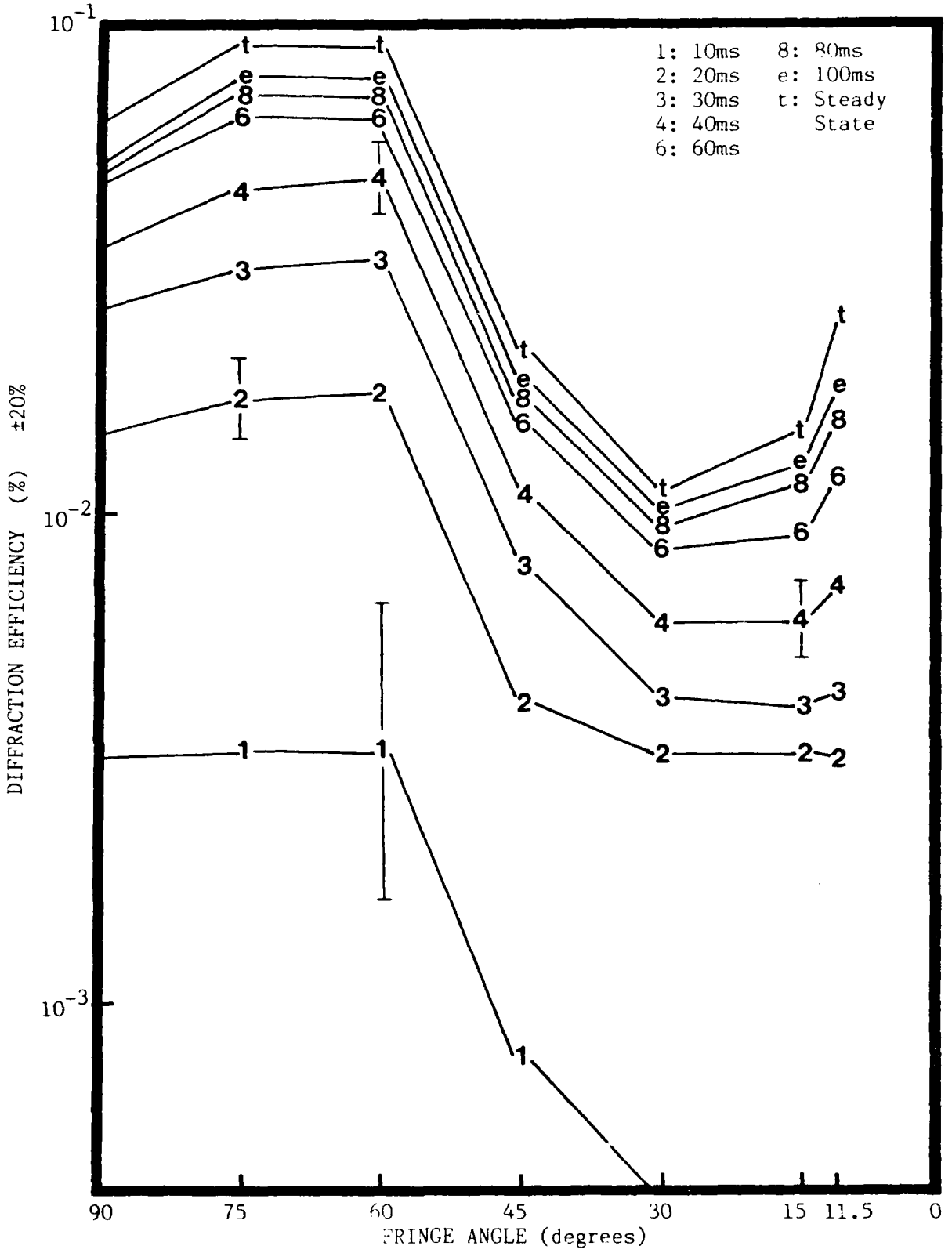

Figure 31. Diffraction efficiency versus fringe angle: M=0.82, scaled ν, Λ=5μ, horizontally polarized read beam, many write times

AD-A138 099 DEPENDENCE OF HOLOGRAPHIC GRATING FORMATION UPON INTERFERENCE PATTERN ORI..(U) AIR FORCE INST OF TECH WRIGHT-PATTERSON AFB OH SCHOOL OF ENGI.. C L MATSON 2/2

UNCLASSIFIED DEC 83 AFIT/GEO/EE/83D-4 F/G 20/6 NL

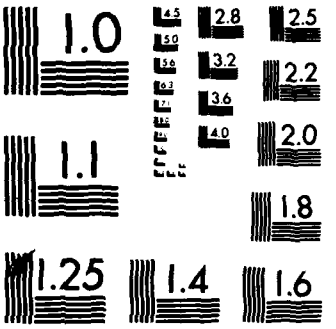

MICROCOPY RESOLUTION TEST CHART
NATIONAL BUREAU OF STANDARDS-1963-A

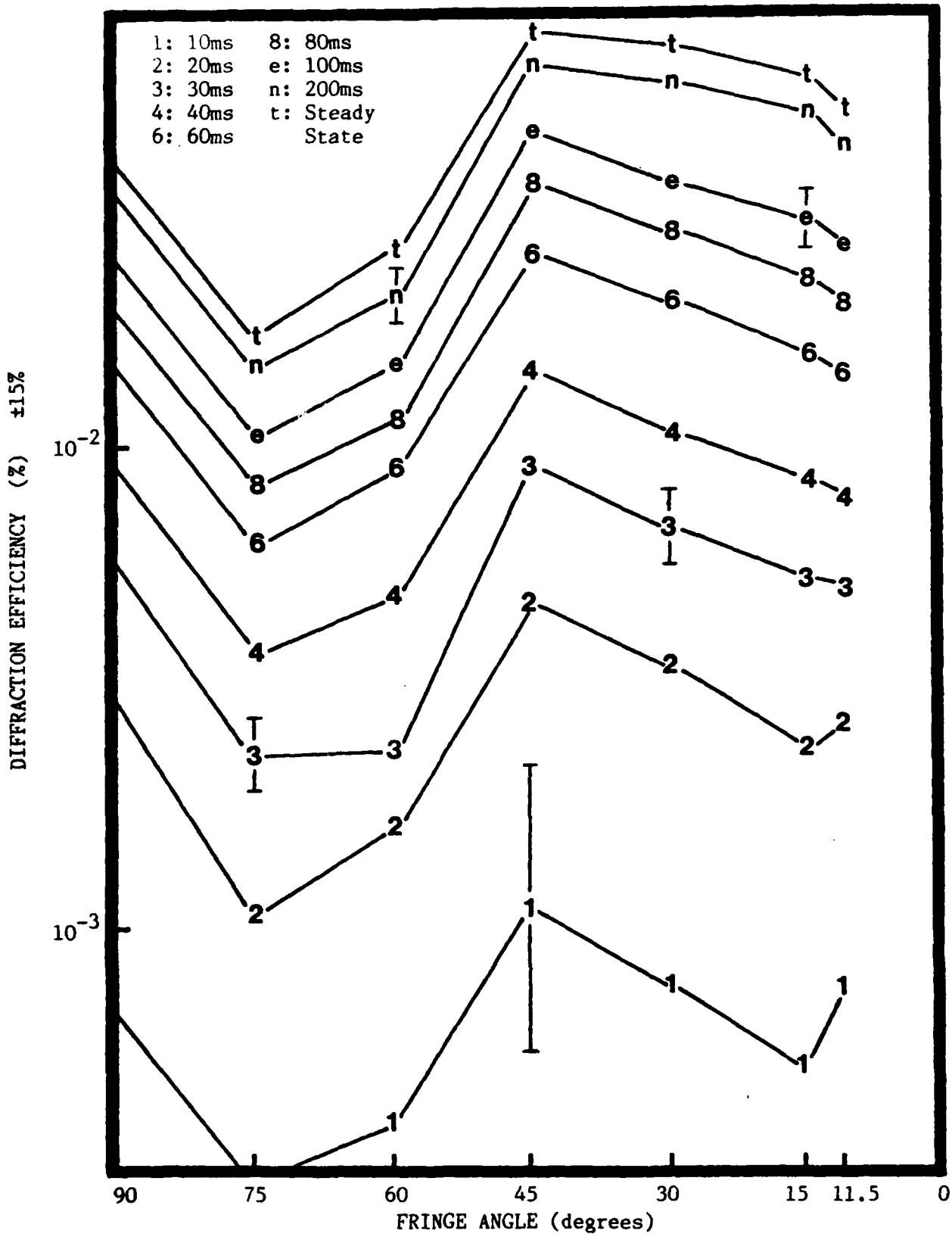

Figure 32. Diffraction efficiency versus fringe angle: M=0.82, scaled V, Λ=3μ, vertically polarized read beam, many write times

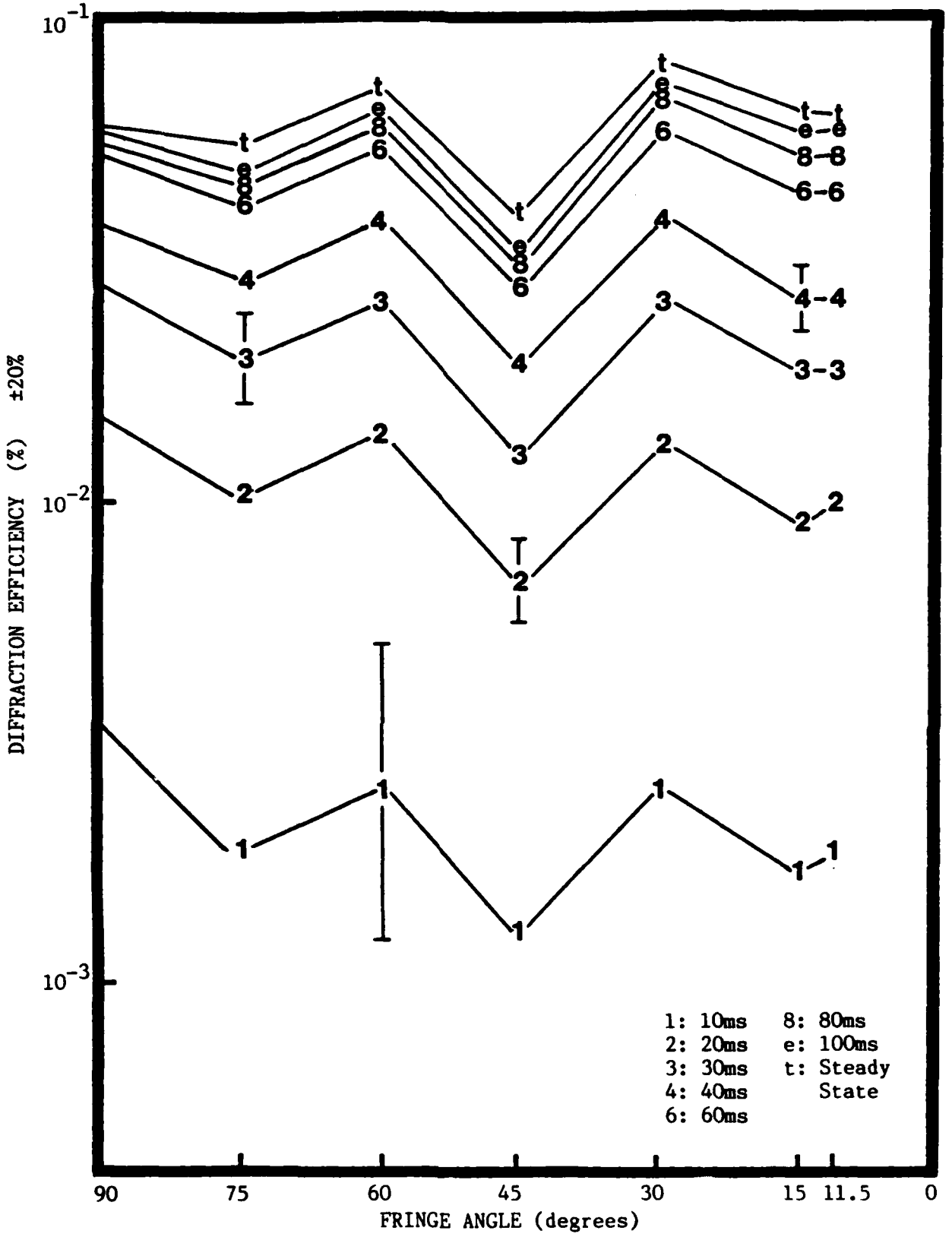

Figure 33. Diffraction efficiency versus fringe angle: M=0.82, scaled V, Λ=5μ, unpolarized read beam, many write times

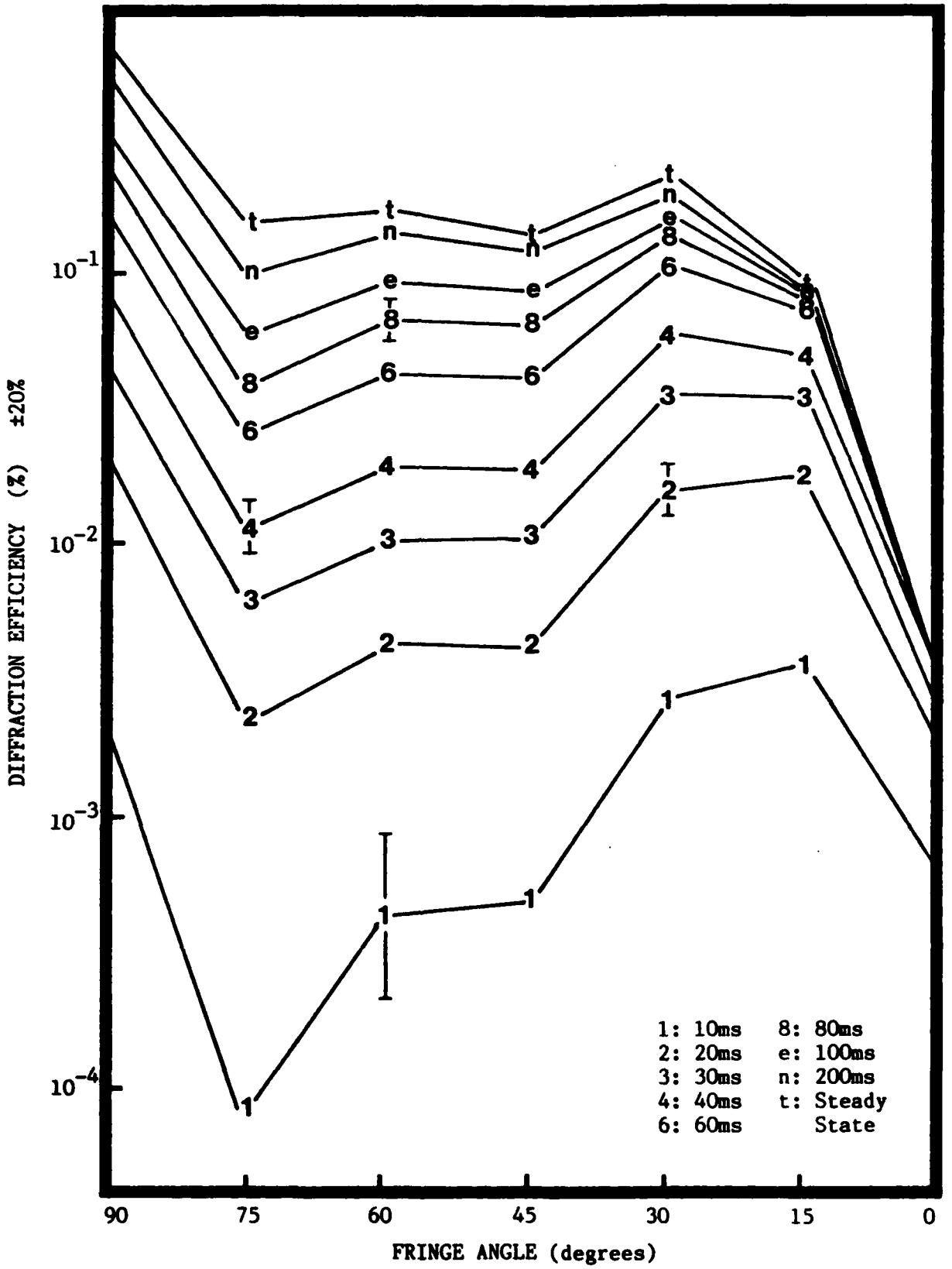

Figure 34. Diffraction efficiency versus fringe angle: M=0.82, V=3kV, Λ=5μ, vertically polarized read beam, many write times

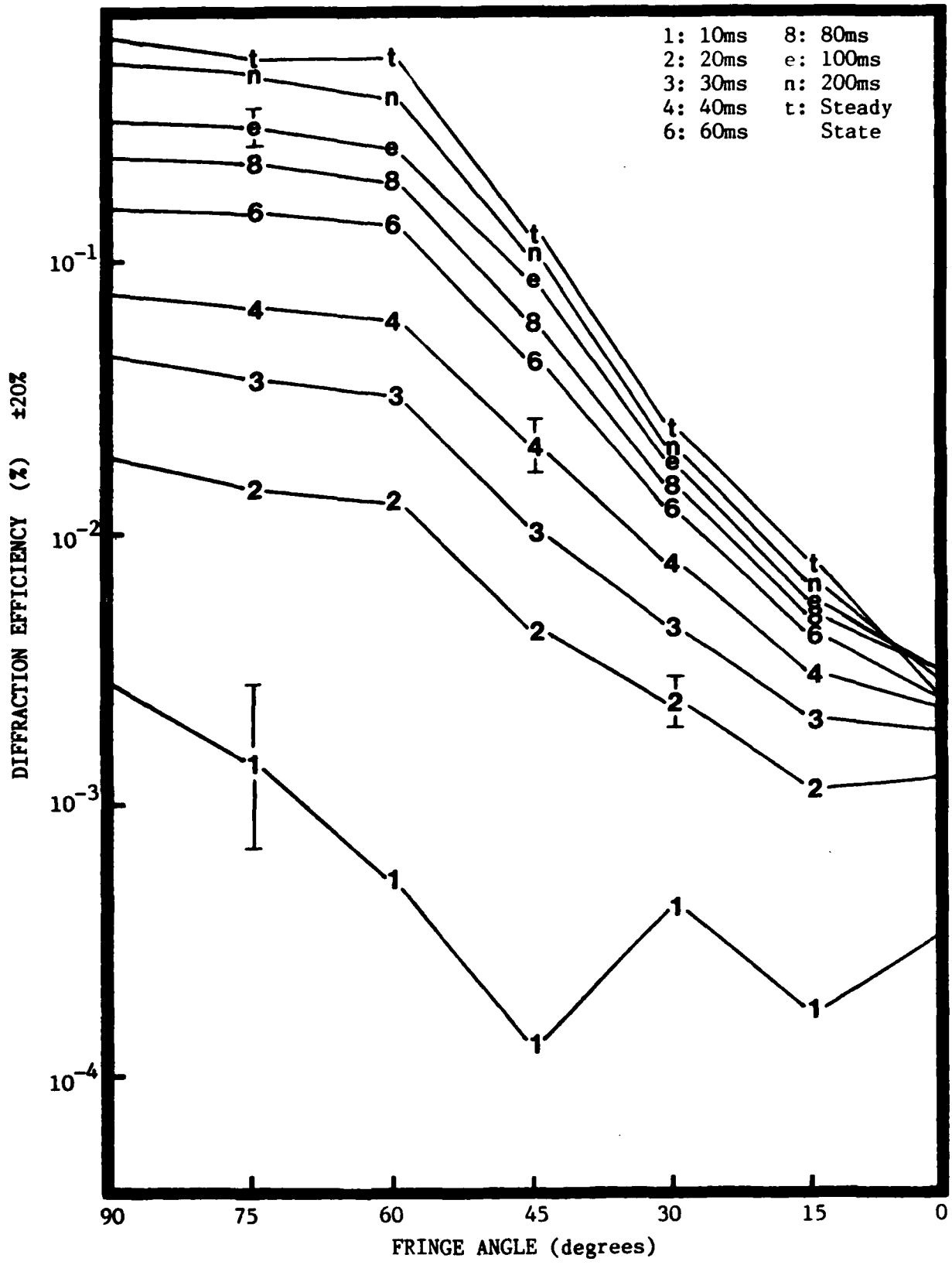

Figure 35. Diffraction efficiency versus fringe angle: M=0.82, V=3kV, Λ=5μ, horizontally polarized read beam, many write times

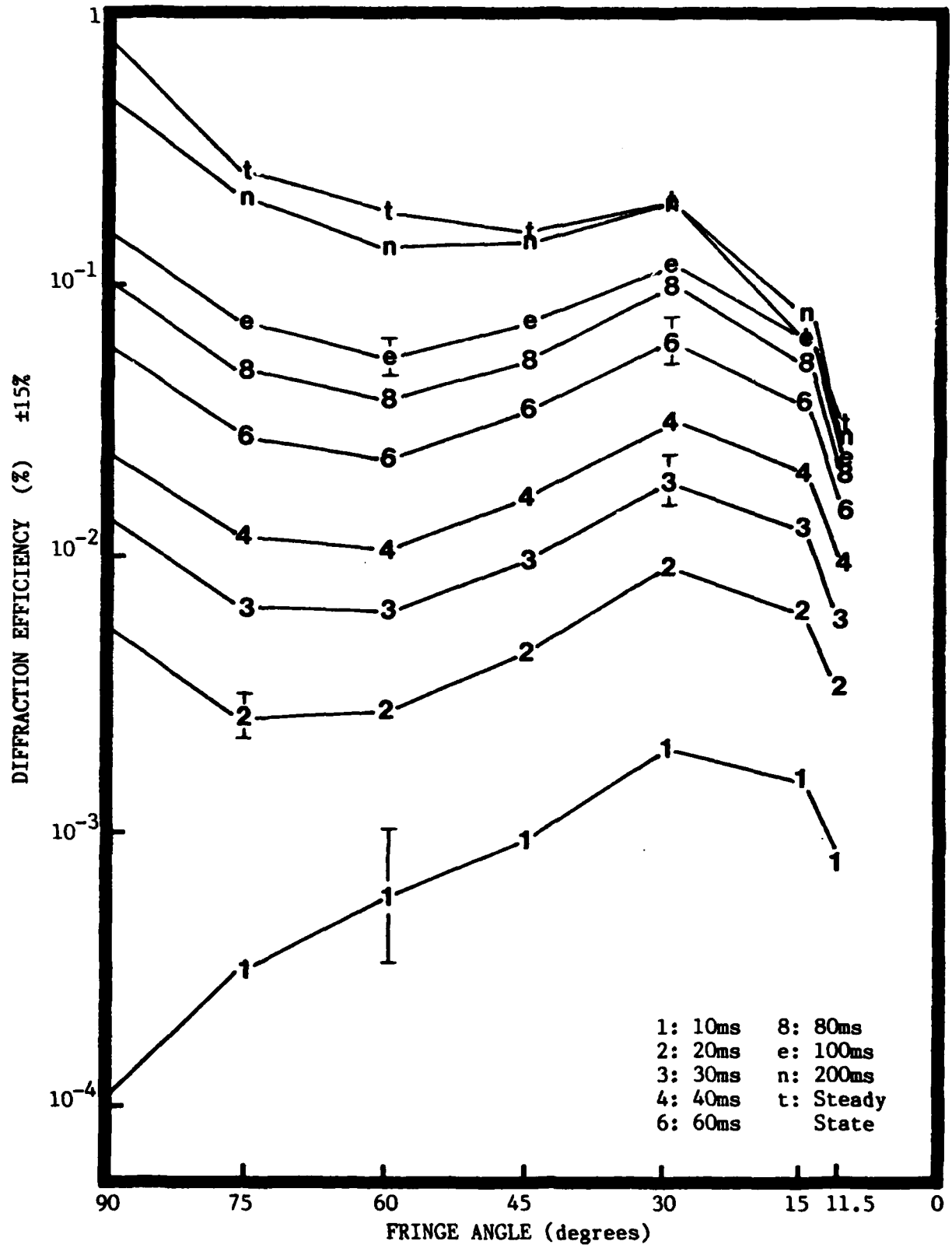

Figure 36. Diffraction efficiency versus fringe angle: M=0.45, V=5kV, Λ=5μ, vertically polarized read beam, many write times

VITA

Charles Leonard Matson was born on 23 February 1960 in Spokane, Washington. He graduated from high school in Pasco, Washington in 1978 and attended the University of Washington from which he received the degree of Bachelor of Science in Electrical Engineering in June 1982. Upon graduation, he received a commission in the USAF through the ROTC program, and entered the School of Engineering, Air Force Institute of Technology, in June 1982. He is a member of Tau Beta Pi.

Permanent address: 5768 Gross Drive
Dayton, OH 45431

UNCLASSIFIED

SECURITY CLASSIFICATION OF THIS PAGE

REPORT DOCUMENTATION PAGE

1a. REPORT SECURITY CLASSIFICATION UNCLASSIFIED	1b. RESTRICTIVE MARKINGS
2a. SECURITY CLASSIFICATION AUTHORITY	3. DISTRIBUTION/AVAILABILITY OF REPORT Approved for public release; distribution unlimited
2b. DECLASSIFICATION/DOWNGRADING SCHEDULE	
4. PERFORMING ORGANIZATION REPORT NUMBER(S) AFIT/GEO/EE/83D-4	5. MONITORING ORGANIZATION REPORT NUMBER(S)
6a. NAME OF PERFORMING ORGANIZATION Air Force Institute of Technology 6b. OFFICE SYMBOL (If applicable) EN	7a. NAME OF MONITORING ORGANIZATION
6c. ADDRESS (City, State and ZIP Code) Wright Patterson AFB, OH 45433	7b. ADDRESS (City, State and ZIP Code)
8a. NAME OF FUNDING/SPONSORING ORGANIZATION Rome Air Development Center 8b. OFFICE SYMBOL (If applicable) ESOP	9. PROCUREMENT INSTRUMENT IDENTIFICATION NUMBER
8c. ADDRESS (City, State and ZIP Code) Hanscom AFB, MA 01731	10. SOURCE OF FUNDING NOS. PROGRAM ELEMENT NO. / PROJECT NO. / TASK NO. / WORK UNIT NO.
11 TITLE (Include Security Classification) (see reverse)	
12. PERSONAL AUTHOR(S) Matson, Charles Leonard	
13a. TYPE OF REPORT MS Thesis 13b. TIME COVERED FROM _____ TO _____	14. DATE OF REPORT (Yr., Mo., Day) Dec 83 15. PAGE COUNT 103
16. SUPPLEMENTARY NOTATION	Approved for public release: IAW AFR 190-17 LYNN E. WOLAVER Dean for Research and Professional Development Air Force Institute of Technology (AIC) Wright-Patterson AFB OH 45433

17. COSATI CODES		
FIELD	GROUP	SUB. GR.
20	6	

18. SUBJECT TERMS (Continue on reverse if necessary and identify by block number)

Bismuth silicon oxide
Photorefractive
Electro-optic crystal
Holographic storage
Thick diffraction grating (phase)
Space charge field

19. ABSTRACT (Continue on reverse if necessary and identify by block number)

Bismuth silicon oxide (BSO) is a material which shows good promise for use as a reusable holographic storage medium, with cycle times on the order of milliseconds. When operated without an applied voltage, fringe patterns are weakly recorded through a space charge field in the crystal equally well for all fringe orientations. The fringes are recorded much more strongly in the crystal when a field of 5 to 10 kV/cm is placed across the crystal; however, strength of fringe storage becomes dependent on the orientation of the fringes upon the crystal. Thus, it is necessary to determine how the strength of fringe storage depends upon the fringe angle to fully utilize the advantage of using an applied voltage to enhance crystal performance.

A particularly simple hologram is made by interfering two plane waves, producing a sinusoidal interference pattern with parallel fringes. By measuring diffraction efficiencies of thick birefringent phase diffraction gratings formed in BSO by recording a sinusoidal interference pattern for a variety of fringe angles, the effect of

20. DISTRIBUTION/AVAILABILITY OF ABSTRACT UNCLASSIFIED/UNLIMITED ☒ SAME AS RPT. ☐ DTIC USERS ☐	21. ABSTRACT SECURITY CLASSIFICATION UNCLASSIFIED
22a. NAME OF RESPONSIBLE INDIVIDUAL Matson, Charles	22b. TELEPHONE NUMBER (Include Area Code) (513) 255-5533 22c. OFFICE SYMBOL

DD FORM 1473, 83 APR EDITION OF 1 JAN 73 IS OBSOLETE.

UNCLASSIFIED

SECURITY CLASSIFICATION OF THIS PAGE

Block 11

Dependence of Holographic Grating Formation upon Interference Pattern Orientation in Bismuth Silicon Oxide
(UNCLASSIFIED)

Block 19

fringe orientation upon fringe storage can be determined. This is the approach used in this thesis to analyze the fringe angle dependence of fringe storage in BSO.

Angular dependence of diffraction efficiencies were obtained for several values of parameters such as applied voltage, modulation coefficient of the sinusoidal pattern, polarization of the diffracted beam, exposure times, and spatial frequency. It was theorized that the effect of the voltage on fringe storage would scale sinusoidally as a function of the angle between the applied field and the fringe pattern. This theory proved to be valid for short to intermediate exposure times for the scaling of the growth rates of the space charge field. Polarization of the diffracted beam also significantly affected fringe storage of the BSO crystal. An index ellipsoid calculation based on an approximation for the space charge field in the crystal gave qualitative agreement for the magnitude of the space charge field growth.

END

FILMED

3-84

DTIC